

AD A O 78922

~~LEVEL~~ 12

AD AD-E400 287

CONTRACTOR REPORT ARSCD-CR-79001

BASE FUZE FOR 30MM H.E.D.P. PROJECTILE

A. ANTONUZZI
C. M. CONLON, JR.
AVCO SYSTEMS DIVISION
WILMINGTON, MASS.

W. J. WARREN
ARRADCOM

DECEMBER 1978

DDC
RECEIVED
JAN 8 1980
E



US ARMY ARMAMENT RESEARCH AND DEVELOPMENT COMMAND
FIRE CONTROL AND SMALL CALIBER
WEAPON SYSTEMS LABORATORY
DOVER, NEW JERSEY

DDC FILE COPY

Approved for public release; distribution unlimited.

BEST
AVAILABLE COPY

79 12 6 126

The views, opinions, and/or findings contained in this report are those of the authors and should not be construed as an official Department of the Army position, policy, or decision unless so designated by other documentation.

UNCLASSIFIED

SECURITY CLASSIFICATION OF THIS PAGE (When Data Entered)

18 ARSCD, SBIE

REPORT DOCUMENTATION PAGE		READ INSTRUCTIONS BEFORE COMPLETING FORM	
1. REPORT NUMBER Contractor Report ARSCD-CR-790015	2. GOVT ACCESSION NO. AD-E400 287	3. RECIPIENT'S CATALOG NUMBER	
4. TITLE (and Subtitle) Base Fuze for 30MM H. E. D. P. Projectile	5. TYPE OF REPORT & PERIOD COVERED Final Report 5 Apr - 31 Nov 78	6. PERFORMING ORG. REPORT NUMBER 475778 - 11/31/78	
7. AUTHOR(s) A. Antonuzzi C. M. Conlon, Jr.	8. CONTRACT OR GRANT NUMBER(s) W. Warren DAAK10-78-C-0141	9. PERFORMING ORGANIZATION NAME AND ADDRESS Avco Systems Division / 201 Lowell Street Wilmington, Massachusetts 01887	
10. CONTROLLING OFFICE NAME AND ADDRESS Commander, ARRADCOM ATTN: DRDAR-TSS Dover, New Jersey 07801	11. REPORT DATE 12 December 1978	12. NUMBER OF PAGES 84	
14. MONITORING AGENCY NAME & ADDRESS (if different from Controlling Office) U. S. Army Armament R&D Command DRDAR-PRW-FS Dover, New Jersey 07801	15. SECURITY CLASS. (of this report) Unclassified	15a. DECLASSIFICATION/DOWNGRADING SCHEDULE	
16. DISTRIBUTION STATEMENT (of this Report) Approved for public release; distribution unlimited.			
17. DISTRIBUTION STATEMENT (of the abstract entered in Block 20, if different from Report)			
18. SUPPLEMENTARY NOTES			
19. KEY WORDS (Continue on reverse side if necessary and identify by block number) Base Fuze 30MM H. E. D. P. Projectile Setback energy generator Electrical fuze			
20. ABSTRACT (Continue on reverse side if necessary and identify by block number) This report describes the base fuze design for a 30MM high explosive dual purpose projectile that resulted from an analysis of many fuze concepts. Features of the fuze design were tested and evaluated in the laboratory using simulated gun launch environments. The base fuze design was fabricated and assembled into test projectiles and gun-tested to measure fuze performance. The fuzes functioned in less than 25 microseconds on impacts against aluminum targets at impact angles of 0 to 45 degrees obliquity and at an impact velocity of 600 meters per second.			

404 788

AB

SUMMARY

The program for the investigation of base fuzing concepts for 30MM dual purpose projectiles was conducted in two phases. In the first phase, a matrix of fuze concepts was analyzed with various methods of implementing the five basic elements of the fuze, namely energy generator, energy storage, impact sensor, energy release and detonator. A detailed technical analysis was made of candidate components. A major factor that influenced the selection of fuze components was the very limited volume of a fuze cavity at the base of a 30MM projectile. Six fuze concepts were examined for response time, graze sensitivity, soft target response, size, cost, complexity and development risk. It was concluded that a fuze consisting of a ferroelectric energy generator, a discrete energy storage capacitor, a deformation switch and a wire-bridge detonator had the greatest potential of all the concepts reviewed for satisfying all of the 30MM projectile requirements.

In the second phase of the program, ten test projectiles were assembled with candidate components and housings into WECOM 30 test projectile bodies. Candidate components were selected after a series of laboratory tests were conducted on the energy generator and storage capacitor, considered the most critical elements in the fuze. Performance characteristics were determined empirically through a series of quasi-static and dynamic loading tests. The laboratory tests concluded that a pair of ferroelectric crystal discs depolarized during a setback load for charging a small ceramic capacitor provided an all-fire energy signal with significant safety margin to fire a microdetonator.

Seven test firings were conducted using x-ray pictures before and after target impact to view the condition of the detonator and other fuze components. The pictures showed conclusively that the fuze functioned as designed and responded within 25 microseconds after target impact. All tests were conducted at impact velocities between 626.7 and 658.8 meters/second (2089 and 2196 feet per second) against 0.229 cm (.090 inch) target plates of 2024-T4 aluminum mounted for normal and 45 degree impacts.

Accession For	
NTIS GRA&I	<input checked="" type="checkbox"/>
DEB TAB	<input type="checkbox"/>
Unannounced	<input type="checkbox"/>
Justification	
By	
Distribution/	
Availability Codes	
Dist	Availand/or special
A	

TABLE OF CONTENTS

	<u>Page No.</u>
Introduction	1
Fuzing System Analysis	2
Fuzing System Elements	6
Energy Generator	8
Piezoelectric	8
Ferroelectric	9
Magnetic Induction	9
Electrochemical (Battery)	10
Energy Storage Element	10
Impact Sensor	10
Ferroelectric	11
Piezoelectric	11
Deformation Switch	11
Triboluminescent	11
Energy Release Element	12
Detonator	12
Design Analysis and Discussion	12
Ballistic Specifications	12
Component Analysis	13
Energy Generator	13
Piezoelectric	13
Ferroelectric	20
Magnetic Induction	23
Electrochemical	24
Impact Sensor	25
Ferroelectric	25
Piezoelectric	26
Direct Fire Mode	26
Impact Signal Mode	29
Polarized Polymer Film ..	35
Deformation Switch	35
Selection of System Approach	39

TABLE OF CONTENTS (Concl'd)

	<u>Page No.</u>
Testing of Fuze Concept	46
Laboratory Testing of Energy Generator Concept	46
Purpose of Tests	46
Test Specimens	46
Test Description	47
Test Results and Discussion	49
Gun Tests	58
Purpose of Tests	58
Test Projectiles	58
Calibration Tests	63
Projectile Tests	63
Reliability	75
Hazard Analysis	76
Conclusions and Recommendations	78
Conclusions	78
Recommendations	78
References	79
Distribution List	81

FIGURES

		<u>Page No.</u>
1	Computer model of 30mm projectile for base fuze study	3
2	Stress-time history on 30mm projectile	4
3	Stress on fuze wall	5
4	Base fuze element combinations	7
5	Schematic representation of piezoelectric setback generator	14
6	Short-circuit charge release characteristics versus parallel stress for a ferroelectric material	22
7	Schematic diagram - HPPD fuze	31
8	Impact sensor equivalent circuit, below resonance model	32
9	Typical relation between indicated and actual G-levels for an impact sensor circuit	32
10	Acceleration ratio versus dimensionless circuit parameter	34
11	Schematic diagram of piezoid stack configuration	37
12	Deformation switch concept	40
13	Reference fuzing system concept (system "A")	45
14	Setup for quasi-static tests	48
15	Setup for dynamic tests	48

FIGURES (Cont'd.)

		<u>Page No.</u>
16	Depolarization of PST-5A with 2.02 μ F capacitor	50
17	Depolarization of PZT-5A with 0.0483 μ F capacitor	51
18	Depolarization of PZT-5A with 0.0308 μ F capacitor	52
19	Piezoid test configuration	55
20	30mm base fuze test projectile	59
21	Setup for gun tests	64
22	X-ray picture of test no. 1	68
23	X-ray picture of test no. 2	69
24	X-ray picture of test no. 4	70
25	X-ray picture of test no. 5	71
26	X-ray picture of test no. 6	73
27	X-ray picture of test no. 7	74

TABLES

1	Selected properties for various piezoelectric ceramic materials at room temperature (25°C)	16
2	Relationship of energy to time for an initially charged RC circuit	19
3	Direct-fire piezoid	28
4	Candidate systems	41

TABLES (Cont'd.)

		<u>Page No.</u>
5	Trade-off summary	42
6	Test results of quasi-static tests	56
7	Propellant calibration	65
8	Gun test data	67

SYMBOLS

A	-	area
C	-	capacitance
d_{33}	-	piezoelectric charge constant
D	-	diameter
E	-	energy
F_n	-	natural frequency
g_{33}	-	piezoelectric voltage constant
G_a	-	actual or input acceleration
G_i	-	indicated acceleration
h	-	height, overall
K	-	slope of acceleration - time forcing function
K_3	-	relative dielectric constant along poling axis
L	-	length
P	-	polarization
R	-	resistance
S_o	-	circuit output voltage sensitivity
S_{oc}	-	open-circuit sensitivity of piezoelectric impact sensor
S_q	-	charge sensitivity
T	-	risetime
t	-	time
V	-	voltage

SYMBOLS (Cont'd.)

V_t	-	trigger circuit threshold voltage
v	-	shock wave velocity
W	-	weight of load mass
ϵ_0	-	permittivity of free space
ρ	-	density
δ	-	stress
m	-	mass
p	-	piezoid
s	-	shunt
opt	-	optimum

INTRODUCTION

Shallow cone shaped charge (SCSC) liners have been demonstrated to exhibit much less spin sensitivity than conventional shaped charge liners. Spin compensation (fluting) is not required making them attractive from both performance and cost standpoints. However, in order to maximize performance, a base fuze is preferable to the conventional nose mounted fuze with a spitback element. A base fuze configuration removes high density components from in front of the liner, but more importantly it eliminates the need for a spitback tube. Conventional spitback tubes actually degrade performance by eliminating jet forming material from the important Apex area of the liner.

In addition to locating the fuze in the base of a high explosive dual purpose (HEDP) projectile, superquick functioning is desired. The required response time is a function of the geometry of the projectile and the striking velocity, but in general 30 microseconds or less is desired. Graze sensitivity is also needed in an HEDP projectile for the anti-personnel role.

A study was conducted by Avco Systems Division and ARRADCOM under Contract No. DAAK10-78-C-0141 to analyze several base fuze concepts. The main thrust of the study addressed power generating materials and storage methods and target sensing techniques.

The release of this report fulfills the obligations of the following items in the Contract Data Requirements List: A002 Final Technical Report, A005 Preliminary Reliability Report, and A006 Preliminary Hazard Analysis.

FUZING SYSTEM ANALYSIS

This section discusses and analyzes candidate base fuze concepts for 30MM dual-purpose projectiles. Before conducting an in-depth study, the feasibility of a base-mounted sensor was explored by performing a structural analysis to evaluate the magnitude of stress signals and the structural response time of signals at the projectile base.

A computer model of a WECOM 30 projectile modified to house a base initiation base detonating (BIBD) fuze (Figure 1) was designed for the study. The following characteristics of the projectile were included in the model:

Weight in grains

Body	2477
Fuze	420
Cu liner	56
Explosive	291
Cu band	138
Total	<u>3382</u>

Center of Gravity	7.165 cm from nose
Moment of Inertia (pitch)	1.0062 kg - cm ²
Moment of Inertia (roll)	0.2895 kg - cm ²

The structural analysis also included the following assumptions:

Yield strength of nose cap material	= 250,000 kg/m ²
Impact velocity	= 750 meter/second
Target media is infinitely hard	
Projectile impact is normal to target surface	

The computed data from the analysis was plotted in curves for better observation of the base-mounted sensor. Stress-time history curves at the point of impact (point A in figure 1) and at the center of the fuze wall (point B in figure 1) are shown in figure 2. An enlarged scale of the stress on the fuze wall is shown in figure 3. The following observations were made concerning a base-mounted sensor:

- a. Response delay was 16 microseconds.

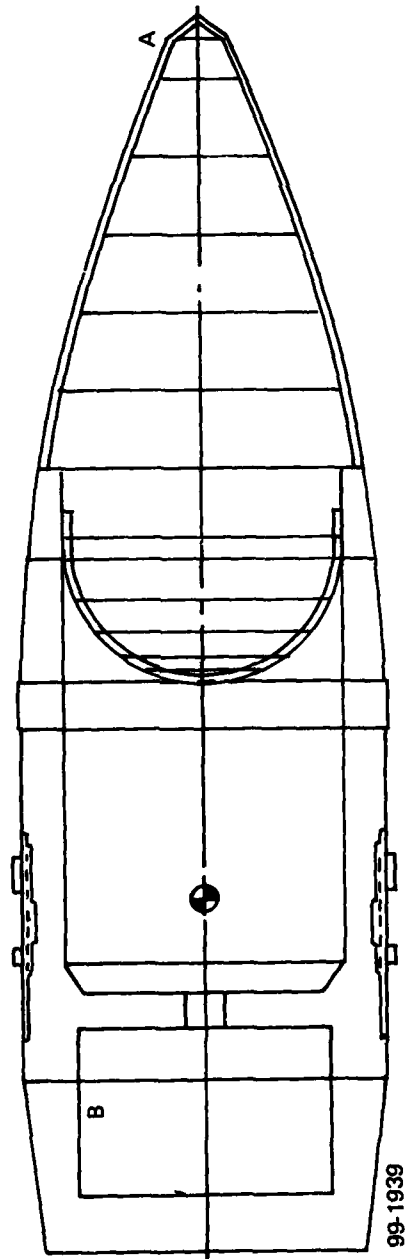


FIGURE 1. COMPUTER MODEL OF 30MM PROJECTILE FOR BASE FUZE RESPONSE STUDY.

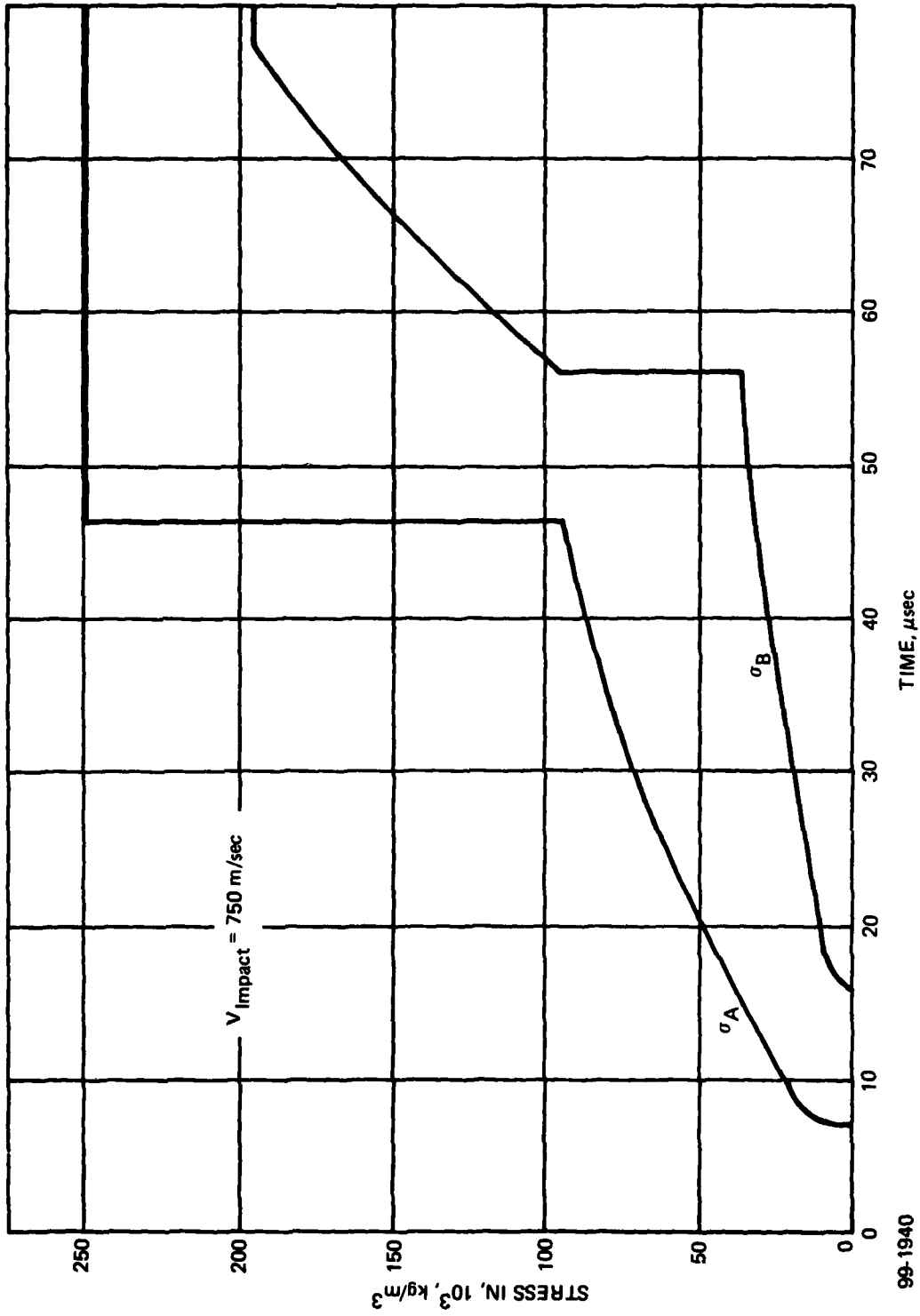
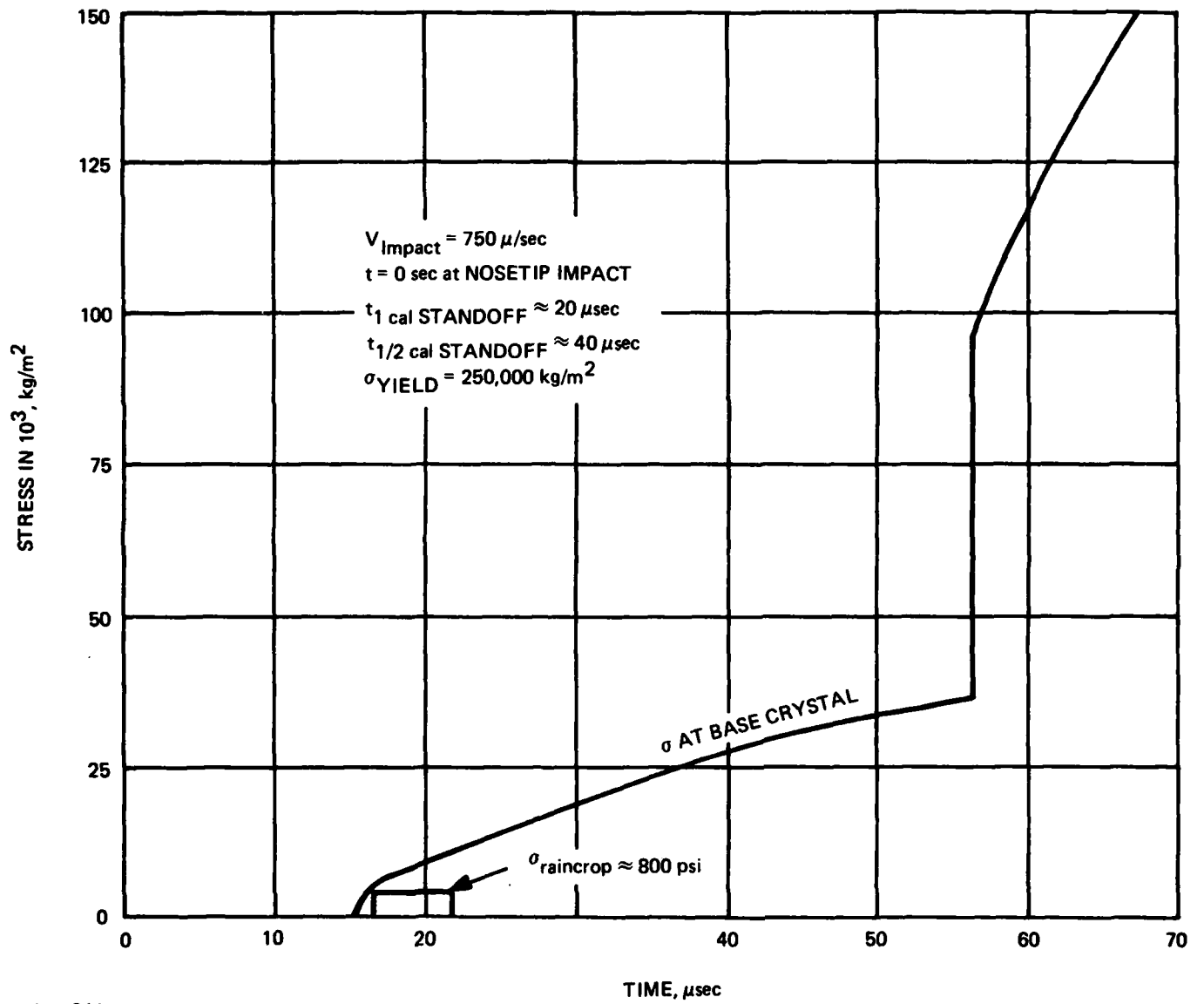


FIGURE 2. STRESS-TIME HISTORY ON 30MM PROJECTILE.



99-1941

FIGURE 3. STRESS ON FUZE WALL.

- b. Until the projectile body hits the target, the stress level was less than $35,000 \text{ Kg/m}^2$ (7000 psi).
- c. The useful stress level for a direct fire crystal power source ($\sim 50,000 \text{ Kg/m}^2$) occurred 57 microseconds after impact.
- d. The early time levels were very close to the levels induced by large raindrop ($\sim 4000 \text{ Kg/m}^2$) indicating a severe design constraint for safing and threshold level for early response.

It was concluded that the response of shock transfer technique for a base-initiated fuze will not provide sufficient standoff for proper operation of a shaped charge warhead.

Since a base-mounted sensor would not provide adequate response time, the fuze study concentrated on a point initiating base detonating (PIBD) fuze design. The following list identifies and defines each of the symbols that are used throughout the technical discussion.

Fuzing System Elements

The basic elements of the fuzing system can be categorized as follows:

- Energy Generator
- Energy Storage Element
- Impact Sensor
- Energy Release Element
- Detonator

Depending upon the kind of devices selected, more than one function may be combined in a single device. Figure 4 summarizes the devices reviewed. The interconnecting lines show possible device combinations that can constitute a total system. The reasons why certain combinations are acceptable, and others are not, will be discussed as the device descriptions are presented.

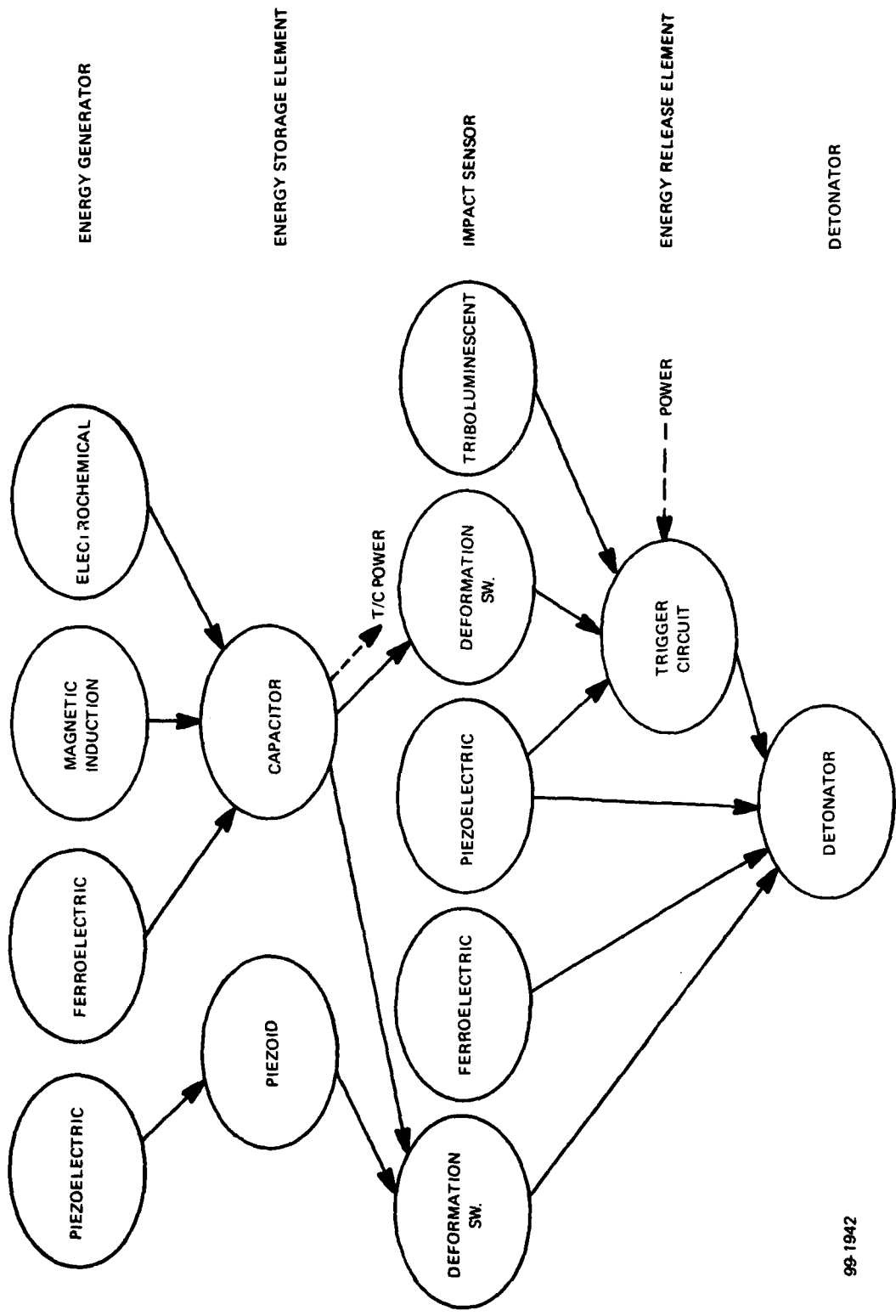


FIGURE 4. BASE FUZE ELEMENT CONSIDERATIONS.

99-1942

Energy Generator

Four types of energy generators are considered:

- Piezoelectric
- Ferroelectric
- Magnetic Induction
- Electrochemical (Battery)

Piezoelectric

This type of generator utilizes the piezoelectric effect possessed by certain materials. This is a linear, reversible effect that can be used to convert mechanical energy to electrical energy during the launch environment (or during impact). A piezoelectric transducer can be used repeatedly, without degradation, provided that its operation is maintained within established stress limits.

Setback acceleration or projectile spin can be used to act on an inertial mass mounted against a piezoelectric element (piezoid). The resulting electrical energy can be stored on the piezoid capacitance. If setback acceleration is used as the input stimulus, some method of preserving the electrical energy after setback is needed since this energy is removed when the piezoid returns to the unstressed state. One technique used on an existing 105MM HEAT-T projectile fuze consists of a shorting switch in the form of a cantilever beam. As maximum setback is approached, the accumulated charge on the piezoid is removed by the closing of the shorting switch. When setback passes its peak level and begins to reduce, the switch opens. Continued reduction of setback produces a charge output (opposite in sign to the original output) as the piezoid returns to the unstressed state. If spin is used as the input stimulus, the shorting switch scheme is not required because the spin environment is sustained from launch to target impact.

The piezoelectric effect is exhibited by certain non-ferroelectric materials, quartz being one example. It is also exhibited by ferroelectric ceramic materials such as lead zirconate titanate (PZT) and lead metaniobate, when polarized by application of an electric

field to electroded surfaces. Some polymer materials can be rendered piezoelectric through a polarizing process, polyvinylidene fluoride (PVF₂) being a prominent example.

Ferroelectric

Ferroelectric materials are crystalline substances which have a spontaneous electric polarization that can be reversed by an electric field. A typical ferroelectric material for transducer applications is lead zirconate titanate in the form of a polarized polycrystalline aggregate structure. This type of material exhibits the linear piezoelectric effect when operated within a limited stress range. When the applied stress exceeds this limit, electric charge in excess of that due to the piezoelectric effect is released to the external circuit. This added output is due to a depolarization phenomena which permanently releases some of the bound surface charge from the electrodes. This is a non-linear and irreverisble effect. However, if structural damage is not incurred, the element can be repolarized and reused. In practical fuzing applications, some structural failure must be anticipated because of the high stress levels required for depolarization; therefore, a ferroelectric transducer generally must be considered a one-shot device that cannot be operated fully prior to its end use. For inspection purposes the degree of polarization can be established by testing in the linear piezoelectric region.

The advantage of a ferroelectric transducer is its relatively large charge release characteristic in comparison to transducers restricted to the use of the piezoelectric effect. One typical application of a ferroelectric element combines it with an explosive device to provide explosive-to-electric energy conversion with the output directly coupled to an electrical load. A distinction must be made between ferroelectric transducers that are directly coupled to the electrical load and those that supply charge output that is stored for subsequent energy release. Different design criteria apply to each case as will be discussed in the design analysis section.

Magnetic Induction

A magnetic induction energy generator basically consists of a permanent magnet, a low-reluctance magnetic circuit completed by a keeper element, and an electric coil. A typical application uses setback to separate the keeper from the remainder of the magnetic circuit. A high reluctance air gap results that reduces the magnetic flux linkage with the coil, thereby inducing a voltage in the coil. When

coupled to a capacitor, useful electrical energy can be stored during setback. A diode is required to retain the energy on the capacitor.

This type of setback generator has been applied to fuzing systems in large caliber applications, for example, the Advanced Batteryless Beehive Fuze. Avco has used a magnetic induction setback generator as the power source for an electrical fuzing system during the HPPD Fuze Program (ref. 1).

Electrochemical (Battery)

Lead-fluoroboric acid batteries are used as power supplies in some projectile applications. This type of battery has a long-term shelf life because it is not energized during storage and self-activates during setback and spin. Its most common use is to power proximity fuze electronics.

Energy Storage Element

Two kinds of energy storage elements are identified in figure 4. Both are capacitive elements, but there is a distinction in the effect they have on the energy stored. As figure 4 shows, if a piezoelectric energy generator is used, the electrical output should be stored on the piezoid element. It will be illustrated in the design section that available energy is lost if the charge output is stored on a shunt capacitor. The other kinds of energy generators use a discrete capacitance to store energy. A ceramic or tantalum capacitor may be appropriate for small caliber application. The specific choice will depend, in part, upon the capacitance value and voltage rating required.

Impact Sensor

Four impact sensing techniques are shown in figure 4:

- Ferroelectric
- Piezoelectric
- Deformation Switch
- Triboluminescent

Ferroelectric

The ferroelectric impact sensor is a one-shot electric charge generator. Its output can be used to directly fire a low-impedance electric detonator if a high-intensity shock wave is transmitted to the element during impact.

Piezoelectric

The piezoelectric effect is used in many impact sensor applications. A mass-loaded piezoid performs a voltage signal function at impact. The output signal functions a trigger which, in turn, delivers stored energy to the detonator. This type of sensor is commonly used in missile fuzing systems, examples being the Minuteman Mk 11C and Mk 12A reentry systems, and the Sparrow and Pershing missiles. In projectile applications the "LUCKY" system is often used. This consists of a piezoid that is stressed at target impact and has its electrical output coupled directly to a detonator.

Deformation Switch

The deformation switch is basically a normally open, single-pole, single-throw switch that closes when the projectile ogive is deformed at target impact. The ogive itself may serve as a part of the switch circuit. Figure 4 illustrates two ways in which a deformation switch may be used. In one case the switch delivers energy directly from the storage element to the detonator. The switch, therefore, serves as both the impact sensor and the energy release element. In the second case the switch is used to transmit an impact signal to the trigger circuit which, in turn, transmits the stored energy to the detonator. With this approach a small amount of energy must be drawn from the storage capacitor to supply the signal to the trigger circuit upon switch closure.

Triboluminescent

In this concept a coating of a special material, referred to as triboluminescent material, is applied to the interior surface of the ogive. When the projectile strikes the target, ogive deformation initiates the radiation of light from the coating. A photosensitive device, mounted in a position to receive the light signal, then supplies a firing signal to a trigger circuit. ARRADCOM is presently researching this technique for potential application to large-caliber projectiles.

Energy Release Element

A trigger circuit is the energy release element required for several of the fuzing approaches shown in figure 4. Its purpose is to release the stored fuzing energy upon receipt of a low-energy triggering signal. It can be powered by the same storage element used to supply the fuzing energy. A typical active element in the trigger circuit is a silicon-controlled rectifier (SCR).

Detonator

The detonators considered here are microdetonator-sized, electrically-initiated types that require from 500 to 1000 ergs all-fire energy. Depending upon the associated fuzing elements, either a low impedance wire bridge (4 to 9 ohms) or a high-impedance, carbon bridge (1000 to 10000 ohms) may be used.

Design Analysis

This section provides the technical basis for the trade-offs among the fuzing system components reviewed. Key performance characteristics are evaluated, component sizes are determined, and their suitability to the 30MM application is discussed. A major factor that influences the selection of a fuzing system is the very limited volume of the fuze cavity. This cavity will have approximate dimensions of 2.03 cm (0.8 in) diameter and 1.4 cm (0.55 in) deep. This volume must contain the arm rotor (or slider), setback and spin locks, and the arm-delay element, in addition to fuzing system components.

Ballistic Specifications

The following ballistic specifications are assumed for the purpose of the present study. The specifications, while not identified for any specific weapon system, are considered to be generally representative for the typical 30MM projectile for a high performance weapon system:

Peak setback acceleration, minimum (g's)	84,000
Spin rate, minimum (RPM)	107,000
Muzzle velocity (m/s)	1,050
Minimum distance to target (meter)	150

Maximum impact velocity (m/s)	1,000
Minimum impact velocity (m/s)	300
Time from setback to impact, maximum (sec)	10

Component Analysis

Energy Generator

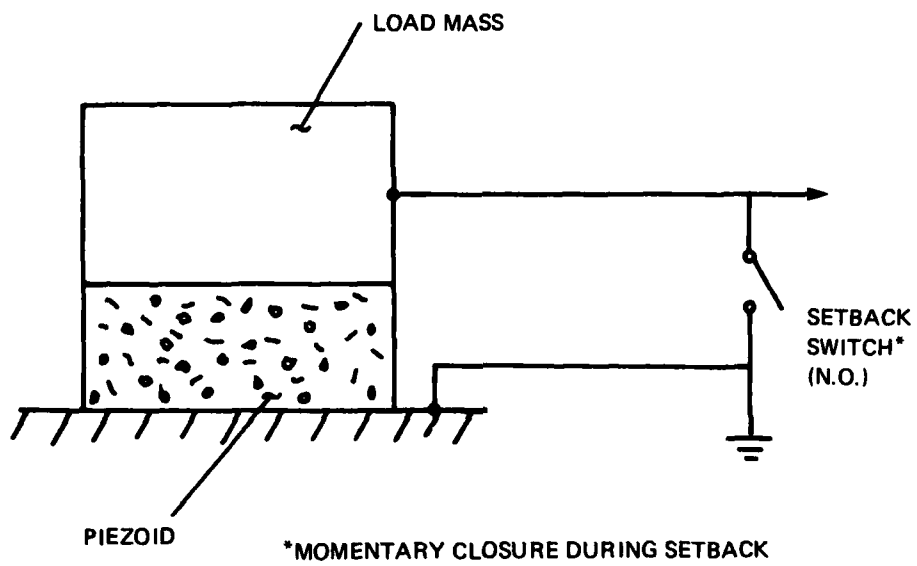
Piezoelectric. The piezoelectric generator may be activated by linear acceleration (setback), or angular acceleration, (spin). In each method the transducer principle is similar. An inertial mass loads the piezoid during setback. The electrical charge output is retained on the piezoid by a suitable means. As discussed under element descriptions, if linear or angular acceleration is used to generate the energy, a device such as a setback switch must be used to prevent the loss of charge as the piezoid returns to the unstressed state following setback. Spin, being present from launch to target impact, does not require an external means to retain the generated charge. Gradual loss of charge, however, will occur during flight due to electrical leakage. The significance of this will be discussed after a design configuration is described.

The functional elements of a piezoelectric generator are shown in figure 5. Volumetric efficiency is a major design criterion for all of the fuzing elements due to the space limitations imposed. The load mass should, therefore, have the highest density possible. A tungsten alloy or depleted uranium are appropriate candidate materials. The piezoid material also has an effect on volumetric efficiency.

The objective in selecting the piezoid material is to obtain the maximum energy output for a given size. Other considerations, such as temperature and time stability, are also important, but a review of the room temperature capability of various materials is the first step in the selection process.

The energy stored in the piezoid is:

$$E = \frac{1}{2} C_p V^2 \quad (1)$$



99-1943

FIGURE 5. SCHEMATIC REPRESENTATION OF A PIEZOELECTRIC SETBACK GENERATOR.

Piezoid capacitance and open-circuit voltage (neglecting mounting losses), respectively, are:

$$C_p = \frac{K_3 \epsilon_0 A_p}{L_p} \quad (2)$$

$$V_{oc} = g_{33} L_p \sigma \quad (3)$$

Substituting the expressions for capacitance and voltage into the energy equation yields:

$$E = \left[\frac{1}{2} \epsilon_0 A_p L_p \sigma^2 \right] \left[K_3^2 g_{33}^2 \right] \quad (4)$$

The elements in the first bracketed term are independent of material characteristics. The second bracketed term is solely dependent on material characteristics and, therefore, may be used as a comparative measure of the energy output of a given material. This characteristic has been computed for several piezoelectric materials and the ratio to the characteristic of PZT-5A (a widely used composition) is presented in table 1 as the relative energy ratio. Other selected material characteristics are also listed.

The materials in table 1 are representative of various compositions from three basic piezoelectric ceramic types: barium titanate, lead metaniobate, and lead zirconate titanate (PZT). Review of the relative energy ratios in table 1 indicates that more energy output capability is provided by the PZT compositions. In this category the PZT-5H composition provides the maximum output capability (30 percent greater than PZT-5A) at room temperature. Review of the pertinent material properties reveals that PZT-5H exhibits a significantly greater change versus PZT-5A over the temperature range associated with projectile fuzing. This is due, in part, to the lower Curie temperature for PZT-5H. For the purpose of sizing a generator, PZT-5A will be used as the reference material.

There is an optimum ratio between the length of the piezoid and the overall height of the piezoid plus the load mass which maximizes the energy output. In establishing this ratio, the following

Table 1. Selected properties for various piezoelectric ceramic materials at room temperature (25°C)

Material	Barium Titanate (Modified)	Lead Metaniobate			Lead Zirconate Titanate							
		4	3	3	1	1	1	2	2	4	4	5
Manufacturer (a)	4	4	3	3	1	1	1	2	2	4	4	5
Mfg. Designation	HS-21 (b)	G-2000	LM-308	LM-391	PZT-5A	PZT-5H	PZT-7	EC-65	EC-66	G-53	G-1500	101
Relative Dielectric Constant, K ₃	1150	250	2000	330	1700	3400	425	1725	2950	720	1700	1700
Curie Temp., °C	125	400	200	500	365	195	350	350	180	330	360	350
Piezoelectric Voltage Constant, e ₃₃ , 10 ⁻³ V-m/N	16	36	13	31	24.8	19.7	39.9	25	20	30	25	23
Relative Energy Ratio	.28	.31	.32	.30	1.00	1.26	.65	1.03	1.13	.62	1.01	.86
Resistivity, 10 ¹⁰ ohm-meters	1.0	0.1	4.0	0.1	10.0							

(a) Manufacturers:

1. Vernitron Corporation
2. Edo Western Corporation
3. General Electric Co.
4. Gulton Industries
5. Linden Laboratories

(b) Production Discontinued

assumptions will apply.

1. The piezoid and the load mass have cylindrical shapes and have equal cross-sectional areas.
2. There is no external capacitance present.

The density ratio between the load mass and the piezoid has an influence on the optimum output ratio. This occurs because the distributed mass of the piezoid produces internal stresses that contribute to the net electrical output. For the materials selected, the density ratio is approximately 2:1. The optimum length ratios for this case and for the case where piezoid mass is neglected are:

$$\frac{L_p}{h} \text{ opt} = \frac{4}{9} h \quad \rho_m / \rho_p = 2 \quad (5)$$

$$\frac{L_p}{h} \text{ opt} = \frac{1}{3} h \quad \rho_m / \rho_p = \infty \quad (6)$$

There are two constraints that affect the design of this kind of transducer. One is the maximum allowable stress for the piezoid material. The way in which the transducer is used requires the use of a shorting switch (except for the spin-operated transducer) that releases electrical charge accumulated during the rising portion of the setback profile. If the piezoid is overstressed during this portion of loading, some depolarization will occur which results in a reduction of the charge output that will subsequently be produced during the decreasing portion of the setback profile. Therefore, a maximum allowable stress must be established.

The generator assembly height constraint and the maximum setback acceleration affect the peak piezoid stress. If, in a particular design, the piezoid is understressed, its cross-sectional area may be reduced with respect to the load mass to increase the output energy. If the piezoid is overstressed, then the load on the piezoid must be reduced to prevent the depolarization problem cited. A second constraint is the maximum allowable output voltage. This limit is a function of the physical design of the generator and its associated circuit.

A representative design has been established for the following constraints and parameters:

Design Constraints -

Allowable stress = $15,000 \text{ kg/m}^2$ (3000 psi)

Output voltage: not to exceed 500 volts

Peak acceleration input = 84,000 g

Design Parameters -

ρ_m = 16.48 gms/cm^3 (0.6 lb/in^3)

ρ_m / ρ_p = 2.0

K_3 = 1700

g_{33} = $24.7 \times 10^{-3} \text{ V-m/N}$

E = 2000 ergs

Quasi-static loading conditions are assumed. Calculations indicate that the resulting overall height of the piezoid, plus the load mass, is 1.96 mm (0.077 in). The piezoid is .86 mm (.034 in) thick and its capacitance is 2225 pF. The diameter of the piezoid is equal to the diameter of the load mass and is 12.78 mm (0.503 in). The output voltage is 424 volts. This is a preliminary calculation that neglects piezoid mounting losses, but it is adequate for trade-off purposes.

By a design process similar to that described for the setback acceleration approach, a spin-actuated piezoelectric generator can be designed. However, all of the piezoelectric generator concepts present a common problem for the 30MM application. An excessively high insulation resistance is required to prevent substantial loss of stored energy during flight.

The leakage resistance requirement can be determined by first considering the relationship between energy loss and the leakage time constant. Table 2 shows the energies available and dissipated for an initially charged RC circuit as a function of a dimensionless time

Table 2. Relationship of energy to time for an initially charged RC circuit

<u>T. O. F.</u> T	Energy Available (% of Original)	Energy Dissipated (% of Original)
0	100	0
0.1	82	18
0.2	67	33
0.3	55	45
1.0	14	86
2.0	2	98

t. o. f. = time of flight
T = time constant of circuit

variable formed by the ratio of time to the RC time constant. For the 10 second maximum flight time specified, it can be seen from Table 2 that if, for example, the leakage time constant is 10 seconds (ratio = 1.0) only 14 percent of the originally stored energy remains at target impact. An acceptable design criterion for the leakage requirement is a time constant that is at least 5 times greater than the maximum flight time. Thus, a minimum of 67 percent of the original energy will be available at impact. The leakage RC time constant then must be 50 seconds minimum. For the piezoelectric generator sizes ($C = 2225 \text{ pF}$), the minimum leakage resistance, therefore, must be 22,000 megohms. The piezoid element is capable of providing this high degree of insulation resistance under laboratory conditions, but this level is not considered practical for the intended application, particularly when other parallel leakage paths in the circuit are included.

The influence of shunt capacitance in conjunction with a piezoelectric energy generator is worth noting. It can be shown that the addition of shunt capacitance for the purpose of increasing the leakage time constant or reducing the voltage level to be compatible with a semiconductor trigger circuit is a very inefficient process. Since the generator produces a fixed amount of electrical charge during a specified mechanical loading, shunt capacitance has the effect of directly reducing the available energy by the ratio of piezoid capacitance to total capacitance.

As an example, consider a shunt capacitance equal to nine times that of the piezoid. The voltage across the parallel combination will be one tenth of that achieved by the piezoid alone. Energy is proportional to capacitance directly and to voltage squared. Thus, increasing capacitance by a factor of ten and decreasing voltage by a factor of ten has the net effect of reducing the energy by a factor of ten.

Ferroelectric. As discussed under the element descriptions, the ferroelectric effect can be implemented in two fundamentally different ways. The element combinations in figure 1 illustrate that one technique is to store the electrical charge output (generated at setback) on a capacitor, for subsequent delivery to the detonator by one of several target sensing methods at impact. The second technique is to use the ferroelectric device as both the impact sensor and the energy generator. In this approach, the ferroelectric element is depolarized due to impact and the electrical charge output is directly coupled to the detonator. This second technique will be

discussed under the impact sensor category.

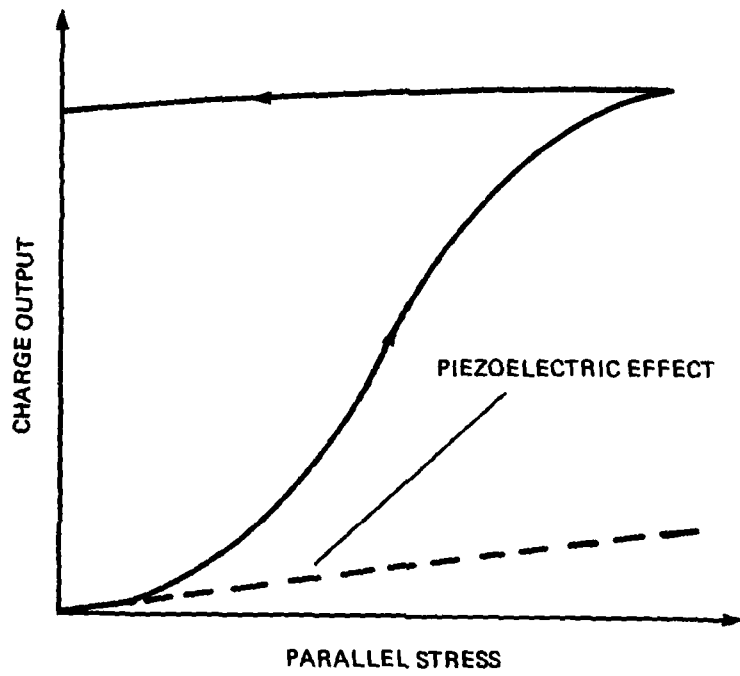
A typical charge release characteristic for a polarized ferroelectric ceramic element under electrical load conditions approaching a short circuit (low voltage gradient) is shown in figure 6 as a function of applied stress parallel to the polarization axis. At low stress levels the linear piezoelectric effect is exhibited. As the stress level is increased, domain switching takes place, resulting in a nonlinear charge release characteristic that substantially adds to the output predicted by the piezoelectric effect. It is this phenomena which permits the use of a relatively small, active element in conjunction with a parallel capacitor to store the released charge.

The parallel capacitor is needed to store the released charge in this type of generator. There are several reasons for this. The relatively large amount of charge released cannot be stored on the ferroelectric element alone due to dielectric breakdown which would be caused by the associated high voltage gradient. Also, since some structural failure of the ferroelectric element can occur caused by the high stress applied, this element should not be depended upon as the energy storage device. A third reason is that a high voltage gradient developed during depolarization tends to inhibit complete depolarization.

The depolarization process is irreversible, therefore, external devices such as diodes are not required to retain the charge on the parallel capacitor during flight. It will be shown that the capacitor will have a relatively large capacitance value. This eases the insulation resistance requirement that was identified for the piezoelectric energy generator.

The concept of generating electrical charge during setback requires application of a high stress level to produce depolarization of the ferroelectric material. The high setback acceleration level associated with the 30MM application allows this technique to be considered.

A material such as PZT-5A will depolarize almost completely at a stress level of $150,000 \text{ kg/m}^2$ (50,000 psi) applied parallel to the polarization axis. This material also has a high polarization of $38 \text{ } \mu\text{C/cm}^2$. Assuming that $30 \text{ } \mu\text{C/cm}^2$ of this polarization is released from a PZT-5A piezoid having a diameter of 0.187 inch, an output of 106 volts across a $0.05 \text{ } \mu\text{F}$ capacitor will result. This represents an energy of 2800 ergs. A piezoid thickness of about 0.076 cm (0.030 inch) will be suitable for this application. The



99-1944

FIGURE 6. SHORT-CIRCUIT RELEASE CHARACTERISTIC VERSUS PARALLEL STRESS FOR A POLARIZED FERROELECTRIC MATERIAL.

250,000 kg/m² stress required can be provided by a high density 16.48 gm/cm³ mass in direct loading of the ferroelectric element. A mass with a diameter of 7.34 cm (2.89 in) and a length of 1.27 cm (0.5 in) will provide the required stress at a setback acceleration level of 70,000 g. As a packaging consideration, it is not necessary for the cross-section of the load mass to be circular. It may also be possible to have other components or structures in the fuzing system act as the load mass, thereby improving the volume efficiency.

The minimum leakage resistance based on a desired 50-second time constant and a .05 μ F capacitance is 1000 megohms. This is considered an acceptable level, particularly if the deformation switch is used as the impact sensor. In this approach, the leakage contribution that would be associated with semi-conductors is eliminated.

A ceramic capacitor may be best suited for this application. The dimensions of a standard 0.047 μ F capacitor rated at 200 volts dcw are 0.76 x 0.76 x 0.38 cm (0.3 x 0.3 x 0.15 in). Leakage resistance for this type of capacitor, well in excess of the required level, is not a constraint. HDL used ceramic capacitors in projectile applications (ref. 2) where the setback acceleration has exceeded 100,000 g. This indicates that a ceramic capacitor can be used as a satisfactory energy storage element.

The charge release characteristic of ferroelectric materials is discussed in several technical papers. Three representative articles are listed among the references (refs. 3, 4, and 5). Ceramic compositions that release their charge due to stress-enforced phase transitions between ferroelectric and antiferroelectric states (refs. 4 and 5) are of considerable interest because depolarization can occur at lower stress levels than is attainable with standard PZT compositions. This would lead to a reduction in the size required for the energy generator.

Magnetic induction. For the purpose of the general trade-off study, a rough estimate of the size of a magnetic induction energy generator can be made by extrapolating from an existing design. The generator used in the HPPD fuze program produced in excess of 30,000 ergs from an overall volume, including the keeper element and housing, of approximately one cubic inch. Assuming a comparable efficiency, it is estimated that a volume of about 52 cc (0.25 in³) is required to produce an output of 2,000 ergs. This is almost equal to the total fuze cavity volume that must also contain the S&A, delay element and storage capacitor. The HPPD generator was not optimized,

but even if the volume scaled for the 30MM was reduced by a factor of two, the size would still be too large. In addition to the size problem, the magnetic induction device is not considered suited for this application because of its complexity and shape constraints in comparison to alternate approaches.

Electrochemical. The major drawback to the application of a battery to this 30MM fuzing system is size. Risetime, which might be suspected as a problem with setback-activated battery, is actually relatively fast, being on the order of 0.03 second (ref. 6). At a muzzle velocity of 1050 m/s (3500 fps), the device is functional at a range of 31.5 meters (105 feet), which satisfies the minimum range requirement.

A size estimate is made for the case where the battery is directly coupled to the detonator. It is established as a guideline that the detonator shall be functioned within ten microseconds following target contact. At the maximum strike velocity of 600 m/s (2000 fps), ogive crush-up will be limited to 0.61 cm (0.24 in) due to this delay. The electrical current density of a battery cell is limited to about 7.75 mA/cm² at the rated cell voltage of 1.2 to 1.8 volts. Therefore, in order to deliver 1000 ergs in 10 sec., a current of 1.05 amperes is required, assuming a maximum detonator resistance of 9.0 ohms. This requires a cell area of 136 cm² (21 in²) and a minimum battery voltage of 1.05 x 9 or 9.45 volts. By a suitable combination of series and parallel cells, a prohibitively large total of 147 cells, each having an area of 6.5 square centimeters is required. (An existing 13 cell stack is 1.9 cm (.75 in) high)). Therefore, direct battery coupling to the detonator is not practical.

A second battery approach uses a capacitor that is charged during flight. Energy to fire the detonator is provided by the capacitor at impact. It is desired to deliver the energy to the detonator in 10 microseconds. During one time constant, 86 percent of the stored energy is delivered from a charged capacitor to a resistive load. Taking the RC time constant as 10 microseconds, at the maximum resistance of 9.0 ohms, the required capacitance is 1.11 microfarads. To deliver 1000 ergs during one-time constant (1000/.86 or 1163 ergs stored), the capacitor must be charged to a voltage of 14.5 volts.

At the minimum cell voltage of 1.2 volts, a total of 12 cells in series is required to provide the required voltage. As previously stated, an existing 13-cell battery is 1.9 cm high. Thus, since battery height is related to the number of cells, the battery is too large for the application.

Impact Sensor

Ferroelectric. A ferroelectric element that is depolarized at target impact can be used in a direct-fire mode under certain conditions. Its principal advantage is that a relatively large amount of electrical charge can be delivered from a small size. In order to utilize the released charge to maximum advantage, a high intensity shock wave must be available to produce depolarization during the transit time of the shock. For a resistive load, if an axial shock wave is transmitted through an axially-poled ferroelectric disk, and if mechanical and dielectric properties of the stressed and unstressed regions are assumed unchanged, then constant current will result during the transit time. Under these conditions, the energy output is:

$$E = \frac{P^2 A^2 \nu R}{L} \quad (7)$$

Equation (7) applies for the condition where the RC time constant is small relative to the shock wave transit time. This is a valid assumption for most practical cases. The preceding equation indicates that energy output is maximized for high polarization, large surface area, high shock wave velocity, large resistance, and minimum disk thickness. The last two factors are subject to a voltage gradient constraint that, if exceeded, can result in dielectric breakdown of the ferroelectric material with a commensurate loss of energy output.

Variations in material properties (e. g., dielectric constant) between the regions behind and ahead of the shock front result in a current output that is not constant as was assumed in the preceding paragraph. Since the current-time integral must be the same for both cases, more energy is produced for the case of nonuniform current output because energy is proportional to the time integral of current squared. Rigorous analysis (ref. 7) and experimental verification indicates that peak current equal to two or three times the average current are produced with representative ferroelectric ceramic materials. Several technical papers related to the subject of ferroelectric ceramic depolarization characteristics are included in references 3, 4, 5, 7, 8 and 9.

An example of a ferroelectric element used in a direct-fire mode is found in the FMU-95B bomb fuze. The element has a diameter of 0.475 cm (0.187 in) and a thickness of 0.076 cm (0.030 in). The material is PZT-5A or equivalent. The load is an Mk 96 detonator with a bridgewire resistance of 2 to 5 ohms and an all-fire energy of 2000 ergs. In the FMU-95B application, depolarization occurs due to a

high-intensity, normal shock generated by the explosive output of a stab detonator initiated at target impact. As stated, this is the most favorable condition for maximizing the energy output from a ferroelectric element. The resulting energy output of this fuze is a minimum of 8000 ergs, which demonstrates the high energy capability that is achievable under the proper conditions.

A ferroelectric sensor sized for a 2000 erg output that would satisfy the microdetonator requirement with an adequate margin has an area equal to one-quarter of the area of the FMU-95B element. This would make the smallest possible sensor; however, it is impossible to achieve the required shock input under the variety of impact conditions that must be considered. Except for the ideal case of normal impact with a rigid target such as heavy steel plate, performance would not be adequate. Graze impact or soft target impact (e. g., packed earth) would not provide the required shock loading, even if multiple sensors were used. Energy output capability drops radically if the input is less than the high-intensity, normal shock condition.

Piezoelectric. Piezoelectric impact sensors can be implemented in two ways. A piezoid can be stressed at impact as the ogive is deformed and the resulting electrical output directly coupled to the detonator. A second technique uses the electrical output of the piezoid as a signal which is coupled to a trigger circuit. The design requirements for the two basic implementations differ. The following paragraphs discuss both types.

Direct fire mode. When a piezoid, directly coupled to a resistive load, is stressed within the linear response region, the energy it delivers depends upon the magnitude and wave-shape of the applied stress. To illustrate several characteristics of this kind of system, the response of a representative piezoid to a ramp-to-constant forcing function will be examined. The influence of the distributed mass of the piezoid can be neglected if the forcing-function risetime is large relative to the transit time characteristic of the piezoid. This will be assumed in the following discussion.

During the ramp portion of the applied stress, the voltage across the load as a function of time is represented by the following equation:

$$V = \frac{\sigma_{\max}}{T} d_{33} A_p R \left[1 - e^{-\frac{t}{R(C_p + C_s)}} \right] \quad (8)$$

for $t \leq T$

where σ_{max} is the maximum stress and T is the risetime.

The energy transferred to the load during the ramp portion of the input is:

$$E_1 = \int_0^T \frac{V^2}{R} dt \quad (9)$$

In addition to E_1 an energy component E_2 is transferred to the load during the constant stress portion of the input. E_2 is generated by the discharge of capacitance ($C_p + C_s$).

A representative case has the following piezoid parameters:

d_{33}	=	370×10^{-12} m/V	(PZT-5A)
C_p	=	600 pF	
D	=	0.635 cm (0.25 in)	
C_s	=	0	

The corresponding piezoid thickness is 0.079 cm (0.031 in) for the reference material. Table 3 presents the total energy transferred to the load (detonator) for various combinations of load resistance and impact risetime. The maximum applied stress is assumed to be $50,000 \text{ kg/m}^2$ (10,000 psi) for all cases to allow the effects of load resistance and risetime to be demonstrated on a common basis. The results of table 3 illustrate the significant influence that load resistance has on energy output. High resistance is needed to obtain the energy required to fire a detonator. Table 3 shows that with a resistance up to 10 ohms (representative of bridgewire detonators) very little energy is produced, even for a fast risetime of one microsecond. Over the range of 1000 to 10,000 ohms (representative of carbon-bridge detonators) substantial energy is produced as long as the risetime is sufficiently fast.

Table 3 illustrates the importance of the risetime characteristic. Therefore, in addition to peak stress, a knowledge of the applied stress-time waveform is needed in order to

Table 3. Direct-fire piezoid

Total Energy Output for Various Values of Load Resistance and Impact

<u>Load Resistance</u> (ohms)	<u>Impact Risetime</u> (microseconds)	<u>Total Energy Output</u> ^d (ergs)
10	1	65
	10	7
	100	1
1000	1	3350
	10	613
	100	65
10000	1	5149
	10	3350
	100	613

a. Piezoid -

diameter = 0.635 cm.
 capacitance = 600 pF
 $d_{33} = 370 \times 10^{-12} \text{ m/V}$

- b. Maximum stress is $50,000 \text{ kg/m}^2$ for all cases.
- c. Risetime under ramp-to-constant applied stress-time profiles.
- d. Total energy includes energy during the ramp portion of applied loading, plus energy due to capacitance discharge of capacitance during constant stress portion of applied loading.

estimate system performance. Since this type of detailed information is generally difficult and expensive to obtain, empirical design techniques are often employed. The "LUCKY" impact fuze, in use for many years, is an example of the direct-fire piezoid technique described.

The ability of a direct-fire piezoid system to function on graze or soft targets is difficult to assess for the reasons presented above. Although the use of several piezoids, distributed to cover various impact directions, would improve the chances of functioning, the cost and complexity are increased.

Impact signal mode. The voltage output that results when a piezoid is stressed can be used as the fuzing signal supplied to a trigger circuit. In this kind of system it is the voltage sensitivity characteristic of the piezoid that is of primary interest, as opposed to the energy output characteristic discussed in the preceding section. The piezoid can be implemented as either a stress wave sensor or as the active element in an inertial sensor with the addition of a load mass.

As a stress wave sensor, the response of the piezoid depends upon the magnitude and wave nature of the stress applied to it. Complex wave relationships exist when the instantaneous stress cannot be assumed uniform throughout the piezoid. The acoustic impedance of the piezoid and structure, plus material interfaces and discontinuities, also have an influence on its response. Insight regarding the response to applied stress can be obtained for simplified loading from expressions such as the voltage response equation presented in preceding section, subject to the restrictions cited. In this case, the resistance (R) and shunt capacitance (C_s) represent equivalent circuit elements for interconnecting lines and trigger circuit input impedance.

If one or more piezoids, used as stress wave sensors, are located in the fuze cavity at the base of the projectile, the need for an electrical connection leading back from the ogive area can be eliminated. However, this adds an acoustic delay of about 15 microseconds for impact normal to the target, corresponding to an additional crush-up of 0.914 cm (0.36 in) prior to detonation (@ 600 m/s).

An impact sensor type consisting of a mass-loaded piezoid is extensively used, particularly in missile groundburst fuzing systems. The Copperhead guided projectile is an example of a system that uses this fuzing approach. The sensor operates by

responding to deceleration at impact. The impact sensor and associated trigger circuit are most commonly applied to missiles and large-caliber projectiles that have rigid nose designs and where soft targets and/or low terminal velocity are specified. Generally, more than one sensor is used to improve performance under oblique impact conditions. Avco designed and tested a system of this type as part of the High-Performance Artillery and Mortar Point Detonating Fuze (HPPD) program (ref. 1) conducted for ARRADCOM. The schematic diagram of the system is shown in figure 7. The system consists of an array of six impact sensors, a trigger circuit using an SCR as the active element, two bridgewire detonators, a power supply capacitor (C_1), and a magnetic induction energy generator. Some of the basic principles related to sensor design and the trigger circuit interface are discussed in the following paragraphs.

One fundamental parameter of piezoelectric sensors is the open-circuit voltage sensitivity. For compression-mode, mass-loaded sensors, the sensitivity can be expressed as follows:

$$S_{oc} = g_{33} L_p W/A_p \quad (10)$$

Typical units for S_{oc} are volts/g. As the preceding equation indicates, the sensitivity is a function of piezoelectric material properties, dimensions, and the load mass. In practice, the calculated sensitivity must be reduced to approximately twenty percent due to mechanical radial constraint of the piezoelectric element in the installed condition. The basic sensitivity applies at frequencies well below the fundamental natural frequency of the sensor. Sensitivity in the region of the natural frequency can be obtained by applying the transmissibility relation for second-order systems to the basic sensitivity equation.

When coupled to an external circuit, the output voltage sensitivity is expressed by:

$$S_o = S_{oc} \frac{C_p}{C_p + C_s} \quad (11)$$

This assumes that the load is essentially capacitive, with the net shunt capacitance C_s consisting of cable capacitance plus capacitance at the trigger circuit input. Restrictions on the preceding equation include an operating frequency that is well-below resonance but above the low frequency roll-off region caused by shunt resistance. An equivalent circuit for a sensor operated well below resonance is shown in figure 8.

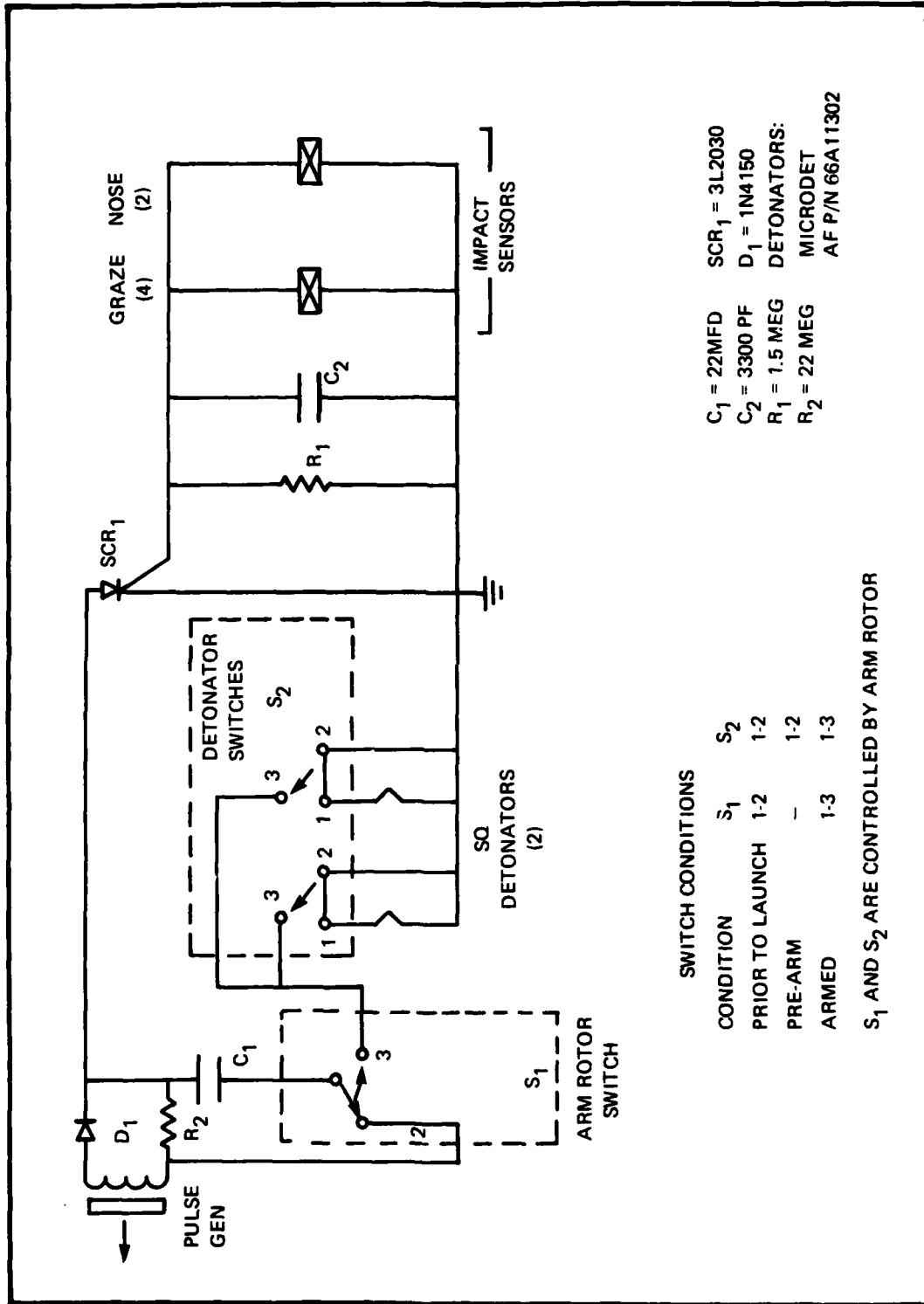
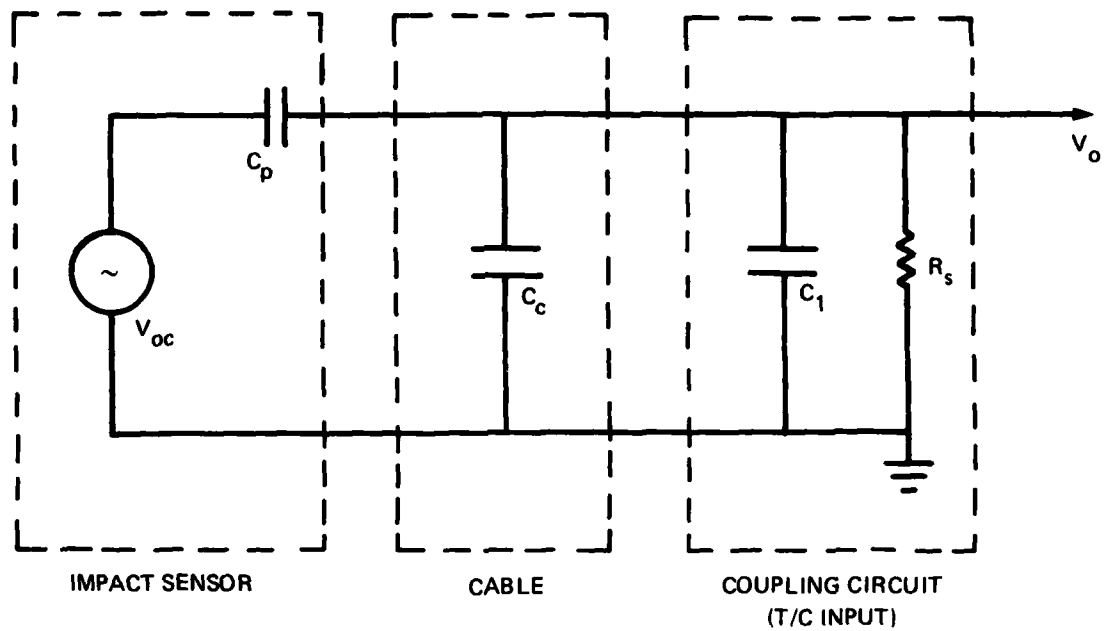


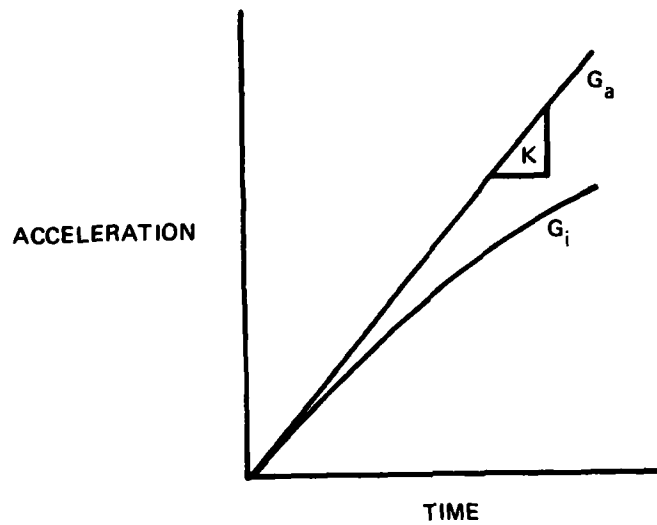
FIGURE 7. SCHEMATIC DIAGRAM OF HPPD FUZE.

99-1945



99-1946

FIGURE 8. IMPACT SENSOR EQUIVALENT CIRCUIT, BELOW RESONANCE MODEL



99-1947

FIGURE 9. TYPICAL RELATION BETWEEN INDICATED AND ACTUAL G-LEVELS FOR AN IMPACT SENSOR CIRCUIT.

In the figure V_{OC} is the equivalent source voltage and is equal to the product of S_{OC} and G_a , where G_a is the input acceleration. The net shunt capacitance (C_s) is equal to the sum of the cable capacitance C_C and the trigger circuit input capacitance C_1 . The trigger circuit input resistance is represented by R_s and V_O is the voltage at the trigger circuit input.

One measure of the dynamic performance of an impact sensor and its associated circuit is the response to a ramp input forcing function. At low rates of applied acceleration, shunt resistance can cause a reduction of the signal available to the triggering element. Figure 9 illustrates this effect for the condition where the natural period of the sensor is small with respect to the ramp risetime. For a ramp input acceleration $G_a(t)$ with slope K , the indicated acceleration level G_i at the triggering element input is as shown in the figure. Sensor response under the described conditions can be generalized using dimensionless parametric ratios. Figure 10 presents the ratio of indicated acceleration to actual acceleration as a function of the input rate and circuit parameters. V_t represents the trigger circuit triggering level; other symbols have been previously defined. For a given circuit, the acceleration ratio is a function of the ramp slope K . An alternate form of the dimensionless abscissa parameters is $K S_q R_s / V_t$, where S_q is the charge sensitivity of the impact sensor. Typical units for S_q are picocoulombs/g.

Figure 10 can be used to illustrate the importance of maintaining a sufficiently high value of the input resistance of the trigger circuit. For example, in the extreme case where R_s forces the dimensionless abscissa ratio to a value of less than 1.0, the triggering level is not reached and the circuit will not function. The combination of circuit parameters and the lowest predicted value of the input acceleration rate should provide a normalized acceleration response approaching 1.0 for satisfactory fuzing system response.

During impact with rigid targets at high velocity, the triggering g-level is reached in a time that is short compared to the natural period ($1/f_n$). For this condition, assuming negligible damping in the sensor, the indicated g-level (G_i) as a function of time (t) is simply:

$$G_i = K \left[t - \frac{1}{2 \pi F_n} \sin \left(2 \pi F_n t \right) \right] \quad (12)$$

Equations 10, 11 and 12 are used in preliminary design to establish

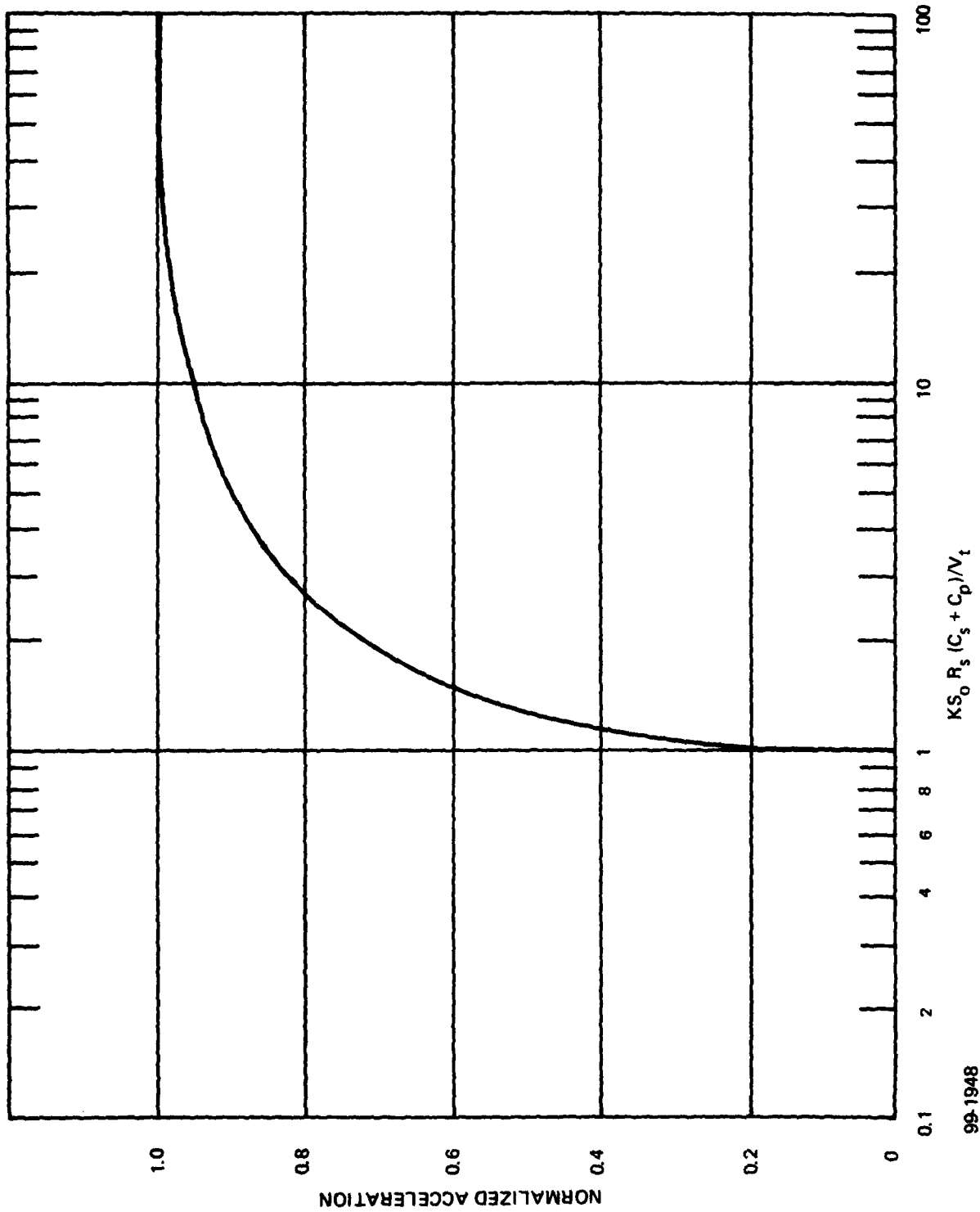


FIGURE 10. ACCELERATION RATIO VERSUS DIMENSIONLESS CIRCUIT PARAMETER.

99-1948

sensor response to the simple, but meaningful, ramp forcing function. If response to more complex forcing functions is desired and if a more rigorous mathematical model of the sensor is appropriate, then a second-order electromechanical equivalent circuit model is used. In this case, the piezoid is represented as a combination of mechanical and electrical circuit elements. Computer-aided solutions for any prescribed forcing function can be determined by using this model.

The techniques described are used to establish the requirements for the impact sensor and trigger circuit input impedance. An important preliminary step in the design of a specific system is the establishment of the extreme impact waveshapes, based on analysis or experiment. A much more detailed knowledge of the impact history is needed in comparison to the other sensor approaches such as ogive-deformation sensors.

Rain sensitivity is an important factor in the use of the piezoelectric impact sensor/trigger circuit system. To attain a fast response, the sensor must have a high natural frequency. However, a high natural frequency can make the system susceptible to premature functioning due to impact with raindrops while the system is in the armed condition. Techniques that may be used to solve this problem include using the highest possible threshold for functioning, and mechanical and/or electrical filtering methods to discriminate between raindrop impact and target impact.

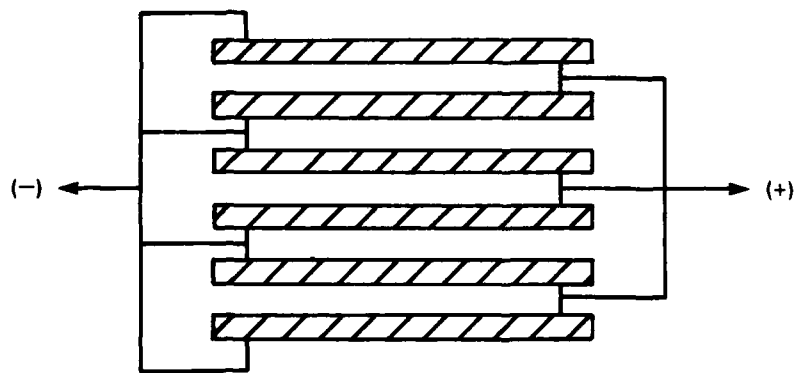
Polarized Polymer film. There has been some interest in the use of polarized polymer film as an alternative to ceramics for fuzing applications. Accordingly, a brief review of this topic is presented.

Polymer films have received considerable attention in recent years for use in commercial and military applications (refs. 10 through 20). The piezoelectric, pyroelectric, dielectric, and nonlinear optical properties of certain polymer materials have been investigated for applications such as electrical resonators (ref. 18), electroacoustic transducer (ref. 12) (e. g., microphones and speakers), and fuzing elements (refs. 11, 20). In particular, polyvinylidene fluoride (PVF₂) has been studied as a fuzing element because of its comparatively strong piezoelectric activity.

PVF₂ has a piezoelectric charge constant (electrical charge produced per unit force applied) that is approximately 0.1 that of lead zirconate titanate (PZT) ceramic material. To increase

the charge output of the polymer, several independently poled sheets may be stacked as shown in figure 11. The sheets are bonded together with the polarity arrangement indicated in the figure. During mechanical loading, each sheet receives the same force and, with the layers connected in parallel, the charge output is proportional to the number of layers. This is a standard technique used to improve the charge sensitivity of piezoids, particularly materials of low sensitivity such as quartz. It should be noted that the electrical interconnections required in a multilayer stack introduces an added fabrication complexity.

Church, Jenkinson, and Esposito have proposed a laminated polymer film transducer contoured to the interior surface of an ogive. In concept, it would serve as an impact sensor that could be used to provide a triggering signal or to provide direct energy transfer to initiate an electric detonator. In conjunction with this concept, tests were conducted (ref. 20) using 1 cm diameter PVF₂ stack assemblies consisting of 20 to 50 layers of 2.54 mm thick material. The layers were interconnected as previously described. The stack assemblies were provided by the Polymers Division of the National Bureau of Standards (NBS) at Gaithersburg, Maryland. A series of reverse ballistics tests were conducted in which the stack under test was sandwiched between steel plates. Flat-nosed WECOM-30 projectiles, having a muzzle velocity of 600 m/sec were fired into the stack assembly and the output voltage developed across a four-ohm resistive load, which is representative of a bridgewire detonator, was monitored. The electrical energy output was approximately 10^5 ergs for the 30 cm² stack area. The above result cannot be directly translated into muzzle performance predictions. The large stack area (intended to approximate the ogive area of a 30MM projectile) combined with the inertial backing (steel plate) and impact parallel to the stack axis with a high density slug at high velocity contribute to maximizing the energy output. When the PVF₂ stack (or any piezoid) is directly coupled to an electrical load, the energy transferred depends upon both the total amount of charge output and the time during which the charge is released. Maximum charge and minimum transfer time produce the maximum energy output. This point is illustrated by means of a simple example. Assume that the same quantity of electrical charge is supplied to a resistive load during two tests with the only difference being the time scale. Energy is a function of the current squared and the first power of time. Therefore, if in the first case a charge is supplied during a time t , and in the second it is supplied during $10t$, then the energy produced in the first case will be ten times that of the second.



99-1949

FIGURE 11. SCHEMATIC DIAGRAM OF PIEZOID STACK CONFIGURATION.

Returning to the ogive-contoured PVF₂ stack concept, it is evident that all portions of the stack cannot be loaded simultaneously upon target impact. Therefore, significantly less output will result in comparison to the reverse ballistic test cited. Several other factors also tend to reduce output energy. Impact with softer targets will reduce the output because the loading rate and the peak load will be diminished. Since a large inertial backing cannot be provided in the ogive area because of its interference with shaped charge jet formation, energy output will be reduced further. The direction of load application will not be, in general, normal to the stack laminations. This not only will reduce effectiveness but also could damage the stack and produce shorting between laminations before the energy transfer is completed.

The tests reported are a definite step forward in helping to form a performance data base for PVF₂ as an energy generating component, but how this material would perform under actual fuzing conditions is not clear at this time.

Several other issues exist regarding the application of this new material to fuzing:

- The effects of long-term storage, particularly under field conditions, are not known.
- PVF₂ polymer begins to depole above the relatively low temperature of 100°C. In an ogive-bonded design, aerodynamic heating of the ogive during flight could severely degrade performance.
- PVF₂ polymer has a substantial pyroelectric coefficient and might produce premature detonation due to sudden heating in flight. The thermal time constant of the polymer stack and the electrical time constant of the firing circuit will have an effect on energy transfer during heating.

At present, some fuze-oriented research is being conducted. The Army Research Office is currently sponsoring study of PVF₂ at NBS (ref. 21). Techniques for directly applying the polymer by spraying are being investigated.

Thus, the status of polymer film technology for fuzing applications leads to the conclusion that several fundamental areas require further study before a specific mission application can be addressed.

Deformation switch. A deformation switch can be used as an impact sensor either to transmit stored energy directly to the detonator or to provide switch closure as a part of a low-current circuit that transmits a firing signal to a trigger circuit.

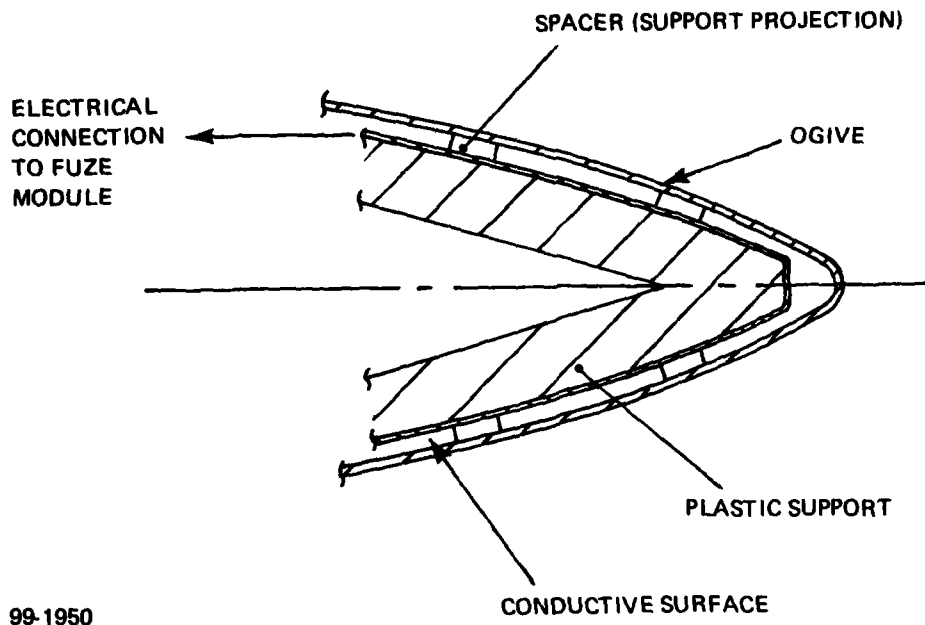
There are several ways in which the deformation switch concept can be implemented for the 30MM application. One method is illustrated in figure 12. It consists of a plastic support with a thin conductive metallic layer applied to the outer surface. The conductive layer is one of the switch contacts. The other contact of the switch is the inner surface of the ogive. An insulated electrical wire connects the conductive layer to the firing circuit in the fuze cavity. The electrical return path is through the ogive and projectile body. Insulated standoffs center the conductive layer with respect to the ogive. The spacing between the contact surfaces can be on the order of 0.25 cm. The contour of the assembly allows the switch to function on graze impacts, provided the required ogive deformation occurs. A switch of this type, combined with a firing circuit having a short time constant, offers the potential for fast operation that will maximize the standoff distance for optimum shaped charge effectiveness.

Selection of System Approach

A variety of fuzing system elements for application to a 30MM base fuze were discussed in the preceding paragraphs. Table 4 presents six representative systems, designated "A" through "F", that consist of various combinations of these elements. The reasons why particular elements are combined were also discussed previously.

A trade-off summary is presented in table 5 for the six systems. A qualitative rating for each system is given for the following evaluation categories:

- Response time
- Graze sensitivity
- Soft target response
- Size
- Cost potential
- Complexity



99-1950

FIGURE 12. DEFORMATION SWITCH CONCEPT.

Table 4. Candidate systems

System Designation	A	B	C	D	E	F
Energy Generator	Ferroelectric	Piezoelectric	Electrochemical	Ferroelectric*	Piezoelectric*	Magnetic Induction
Energy Storage Element	Capacitor	Piezoid	Capacitor	--	--	Capacitor
Impact Sensor	Deformation sw.*	Deformation sw.*	Deformation sw.*	Ferroelectric*	Piezoelectric*	Piezoelectric
Energy Release Element	Deformation sw.*	Deformation sw.*	Deformation sw.*	--	--	Trigger Circuit
Detonator	Wire Bridge	Wire Bridge	Wire Bridge	Wire Bridge	Carbon Bridge	Wire Bridge

*Represents a multiple function element for a given system.

Table 5. System trade-off summary

System	A	B	C	D	E	F
Response Time*	Excellent	Excellent	Moderate	Excellent	Excellent	Good
Graze Sensitivity	Excellent	Excellent	Excellent	Poor	Uncertain	Good
Soft Target Response	Excellent	Excellent	Excellent	Poor	Uncertain	Moderate
Size	Moderate	Moderate	Large	Small	Small	Large
Cost Potential	Low	Moderate	High	Very Low	Very Low	Very High
Complexity	Low	Moderate	Low	Very Low	Very Low	High
Principal Disadvantage(s) or Risk Area(s)	No known prior ammo use	High leakage resistance req'd	Size, cost	Graze sens., soft target resp.	Graze sens., soft target resp.	size, cost, complexity

*Hard target, normal impact

- Principal disadvantage(s) or risk area(s)

System "A" consists of a ferroelectric energy generator, a discrete energy storage capacitor, a deformation switch, and a wirebridge detonator. This system is rated as excellent for hard-target response time because the deformation switch can function at approximately 0.25 cm ogive crush-up and the all-fire energy is delivered to the detonator in less than one microsecond. Graze sensitivity and soft target (e. g., packed earth) responses are rated as excellent because it is expected that sufficient ogive deformation will occur in these cases to function the contoured deformation switch. The size of this system is considered moderate. The fuze cavity components (ferroelectric generator, capacitor, and detonator) that were sized for this application are compatible with the available volume. It is considered that the system has a low-cost potential for a high-performance base fuze. The deformation switch is simple and is suited for efficient high-volume production. The electrical connection extending from the deformation switch to the fuze cavity would require specific attention, if mass production were implemented, to assure that it could be installed reliably and economically. The ferroelectric element in very large production quantities costs approximately ten cents and the capacitor could be selected from a standard ceramic series. The system is not complex and requires only a few parts. However, there is no fuze in production or in development that uses this sytem approach. Therefore, some risk must be associated with the concept, although the basic principles are considered sound and the risk is considered minimal. It is concluded that this approach has the greatest potential of all the systems reviewed for satisfying all of the 30MM requirements.

System "B" contains a piezoelectric energy generator with the piezoid acting as the energy storage element. A setback-operated switch is needed so that the electrical charge will be retained after setback. The impact sensor is a deformation switch and a wirebridge detonator is used. The response time, graze sensitivity, and soft-target response are comparable to system "A". The size is moderate; although the generator is larger than the system "A" version, a separate storage capacitor is not required. The major disadvantage of this system is the high insulation resistance required which is why this concept is not considered suited for the 30MM application.

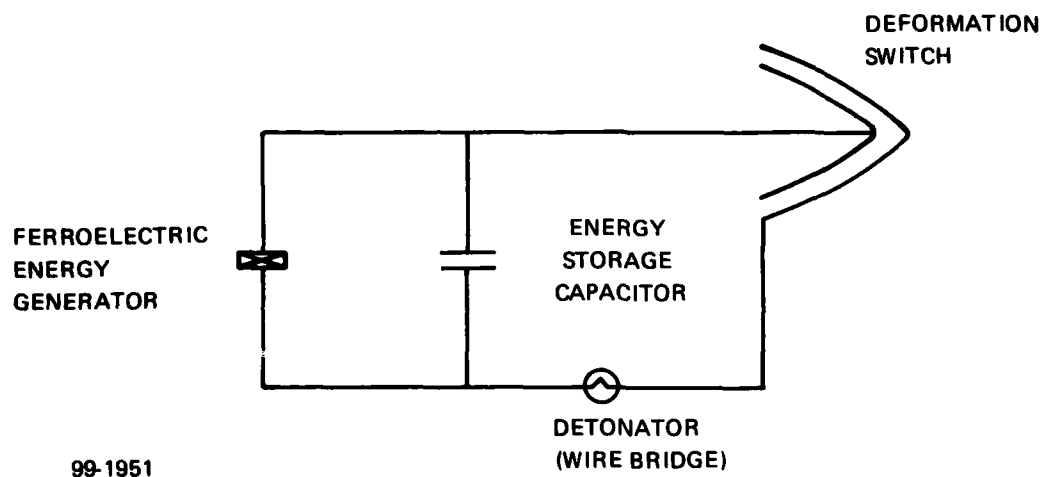
System "C" uses a battery as the energy generator. It has been shown that a battery sized to provide the required function would be too large relative to the volume available in the fuze. Therefore, this reason alone is sufficient to rule out a battery-powered system.

System "D", which uses the depolarization phenomena associated with a ferroelectric element to directly fire a detonator at impact, will not perform satisfactorily for off-normal impacts or for soft-target impacts. The performance limitations of this system eliminate it from further consideration in this application.

System "E" is the "LUCKY" approach that uses the output of a piezoid at impact to directly fire a carbon-bridge detonator. Uncertainty regarding graze sensitivity and soft-target performance are the major reasons for rejecting this system as the primary approach. It is regarded as the second-ranked approach. The feasibility of system "E" would be based on the number of sensors needed to provide coverage for the full range of impact conditions. Obviously, the greater the number of sensors needed, the less desirable this system becomes.

System "F", containing a magnetic setback generator, trigger circuit, and piezoelectric sensor, is comparable to the HPPD fuze system. However, it is not appropriate for the 30MM application. It is the largest, most complex, and costly of the approaches considered.

A schematic diagram of the reference fuzing system approach described, system "A", is shown in figure 13. The involvement of the safing and arming mechanism in this circuit is not illustrated. There are several ways that the S&A can contribute to fuzing system safety and fail-safe modes. As a minimum, the S&A should electrically short the detonator terminals during storage and prior to arming. In addition, the detonator can be isolated from the firing circuit prior to arming. Also, the S&A can combine with the deformation switch in a manner that places an electrical short-circuit across the energy storage capacitor at the pre-arm position in the event that a short-circuit failure mode exists in the deformation switch at the time of projectile launch. This will prevent the system from firing upon arming for the shorted deformation switch failure mode.



99-1951

NOTE: S&A SWITCHING FUNCTIONS NOT SHOWN.

FIGURE 13. REFERENCE FUZING SYSTEM CONCEPT (SYSTEM "A").

TESTING OF FUZE CONCEPT

Laboratory Testing of Energy Generator Concept

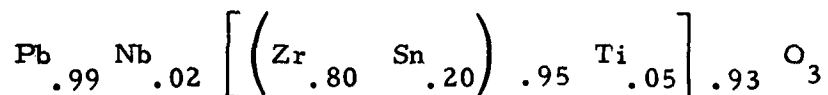
Purpose of Tests

The selected fuze system consisting of a ferroelectric energy generator, an energy storage capacitor, an impact-actuated deformation switch, and an electric detonator required laboratory tests to establish the feasibility of the concept. The laboratory effort was concentrated on the energy generator and storage capacitor combination because these were considered to be the most critical elements in the system and specific performance characteristics had been determined experimentally. The primary objective of the laboratory tests was to determine the capability of the ferroelectric generator concept to produce enough energy during setback to fire a detonator. This was accomplished through a series of both quasi-static and dynamic loading tests in which selected ferroelectric elements were used with various external circuit capacitance values.

Test Specimens

The ferroelectric material used in the majority of the tests was a lead zirconate titanate ceramic composition (commercially designated PZT-5A). The test configuration was a piezoid 0.475 cm in diameter and 0.076 cm thick with fired silver electrodes applied to its flat surfaces. A new piezoid was used for each test.

Limited tests were performed using a modified lead zirconate titanate in the material category designated as PSZT composition. The specific chemical formulation of the material tested was:



The abbreviated notation for this composition is 80/20-5-2 Nb. Each PSZT specimen was a square plate having dimensions of 0.419 x 0.419 x 0.127 cm. The electrodes were evaporated gold. Depolarization of this type of material can be induced by a pressure enforced phase transition from a polarized ferroelectric state to an antiferroelectric state. This material was of interest because it is known that substantial charge can be released at lower stress levels than PZT-5A under hydrostatic loading conditions. The testing was

intended to establish whether there was any benefit associated with the PSZT composition when loaded in the mounting condition presented by the energy generator application (which approaches one-dimensional strain).

Test Description

The test setup used to conduct the quasi-static (or slowly applied) load tests is shown in figure 14. The test apparatus is identified in the figure. The setup contained a hydraulic press with a dial load gauge calibrated using a BLH SR-4, type U-1, load cell. The load transfer blocks were made of hardened steel to prevent deformation under the maximum stress applied ($425,000 \text{ kg/m}^2$). The external capacitor circuit was in parallel with the piezoid and the generated output voltage was measured with an electrometer. The input impedance of the electrometer was high (10^{12} ohms) so that electrical leakage during a test can be neglected.

For better simulation of an actual gun-launch environment dynamic testing was performed using the test setup shown in figure 15. A guided mass weighing 0.675 kg (1.5 pounds), released from a preselected height in a drop test fixture, was used to produce the transient stress loading in the test specimen. A silicone rubber waveshaping pad was included between the guided mass and the load transfer block to provide the desired stress amplitude and risetime. The instrumentation for measurement of the test specimen output was identical to that used in the quasi-static load tests. An accelerometer attached to the guided mass monitored the acceleration-time profile during impact. This information established the force-time and stress-time loads applied to the test specimens. The accelerometer output was fed to a cathode follower. The output of the cathode follower was displayed on an oscilloscope and a photographic record of the applied pulse was obtained for each test conducted.

The quasi-static tests were conducted at two peak stress levels. Some of the test specimens were exposed to the design stress of $250,000 \text{ kg/m}^2$ (i. e., the energy generator will be designed to produce a minimum stress of $250,000 \text{ kg/m}^2$ in the piezoid during setback). Other tests were conducted with an applied peak stress of $425,000 \text{ kg/m}^2$ which corresponds to the maximum capability of the test equipment.

Three external capacitors were used during the test program. Two of the capacitors were mylar types rated at 400 WVDC,

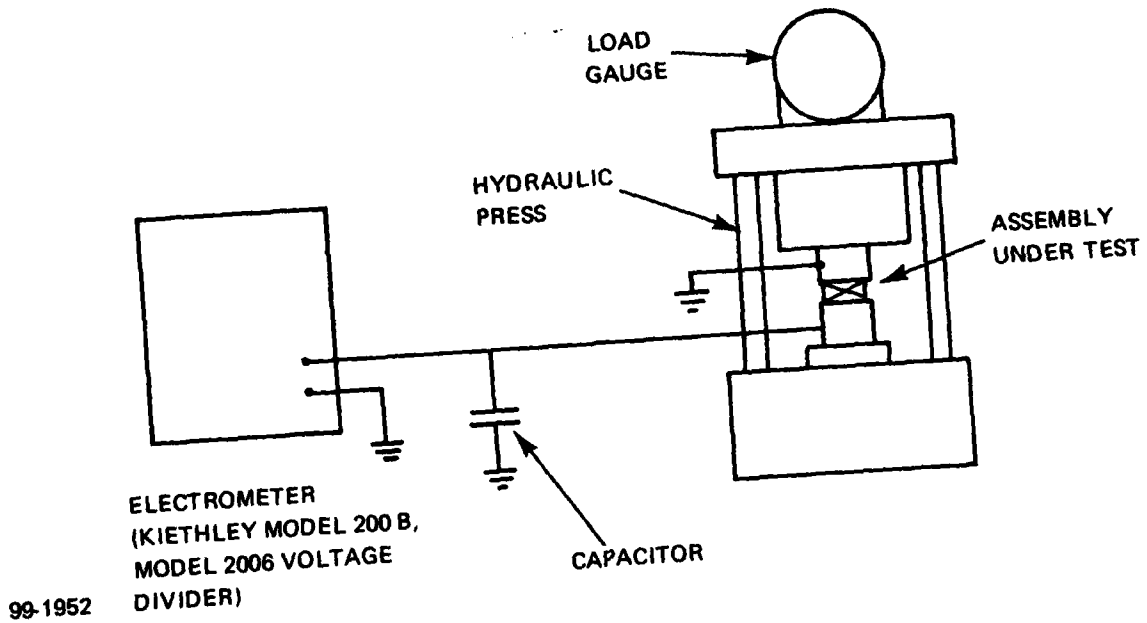


FIGURE 14. SETUP FOR QUASI-STATIC TESTS.

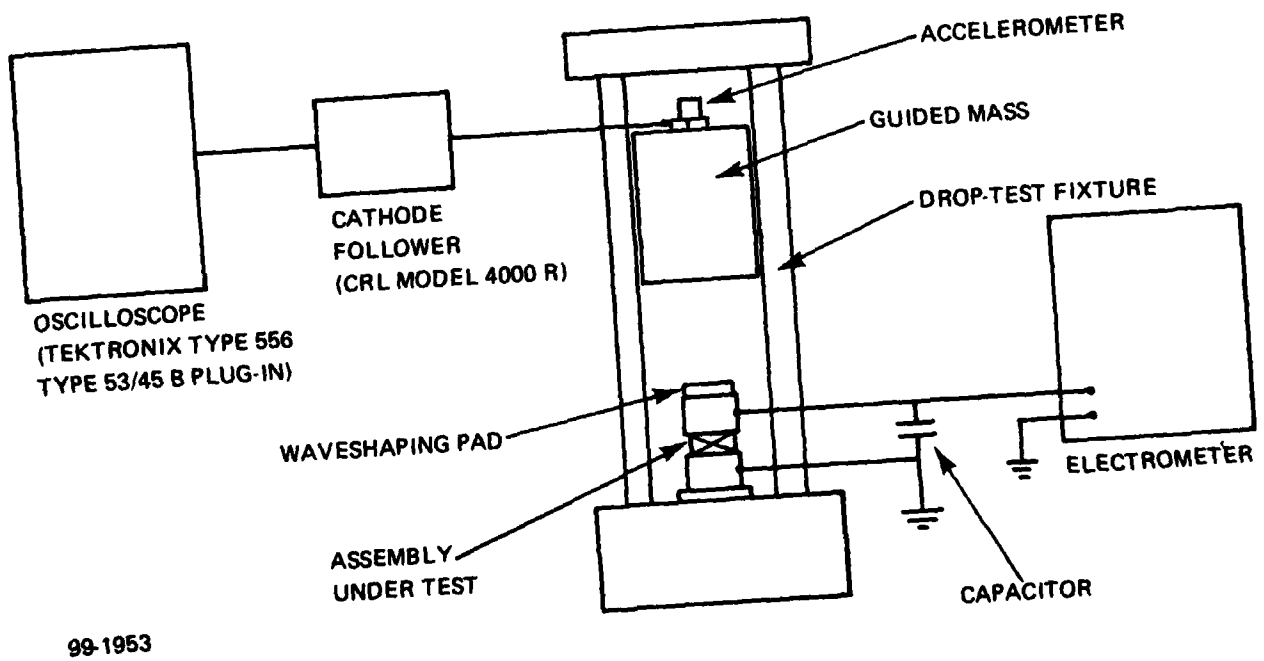


FIGURE 15. SETUP FOR DYNAMIC TESTS.

selected for laboratory reference purpose because of their stability and low-loss characteristics. The measured capacitance values were 2.02 μF and 0.0483 μF . The 2.02 μF capacitor was used to collect charge output under conditions approaching a short-circuit, i. e., low voltage gradient across the test specimen. The 0.0483 μF capacitor was in the capacitance range intended for the fuzing system. The third capacitor used was a ceramic type that has the specific construction chosen for the energy storage capacitor on the basis of its structural ruggedness and small physical size. This test capacitor had a measured capacitance value of 0.0308 μF . It was an Erie type 8131-500-W5R0-333K, having a nominal capacitance of 0.033 μF and a rated voltage of 500 WVDC.

Test Results and Discussion

Test specimen output under quasi-static loading is presented in figures 16 through 18 in terms of loss of polarization versus stress applied parallel to the axis of polarization. Loss of polarization is the electric charge released to the external circuit per unit area of the ferroelectric element and is computed from the following relation:

$$P_r = \frac{CV}{A}$$

where:

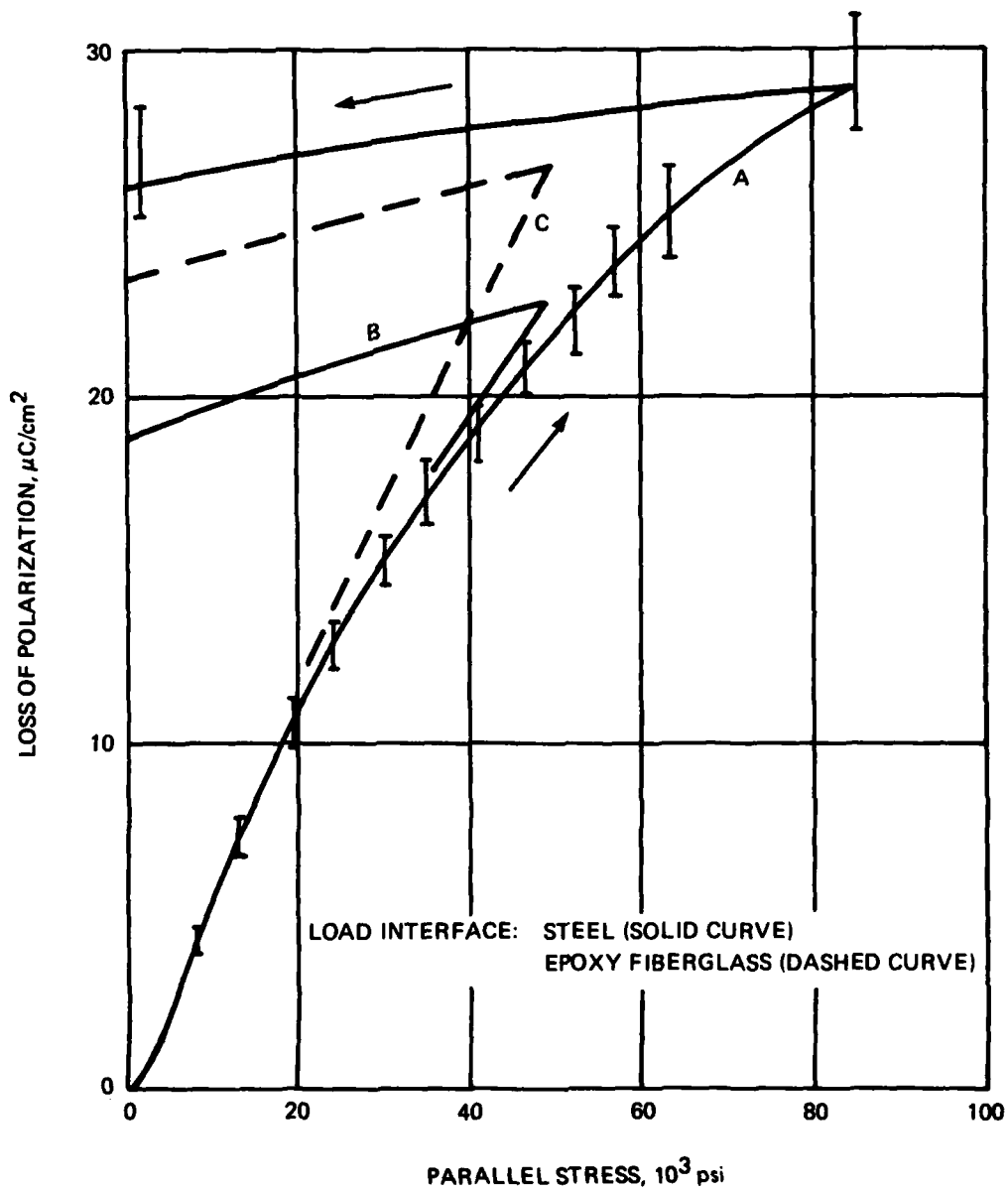
$$P_r = \text{loss of polarization, } \mu\text{C}/\text{cm}^2 \quad (13)$$

$$C = \text{capacitance, } \mu\text{F}$$

$$V = \text{voltage, volts}$$

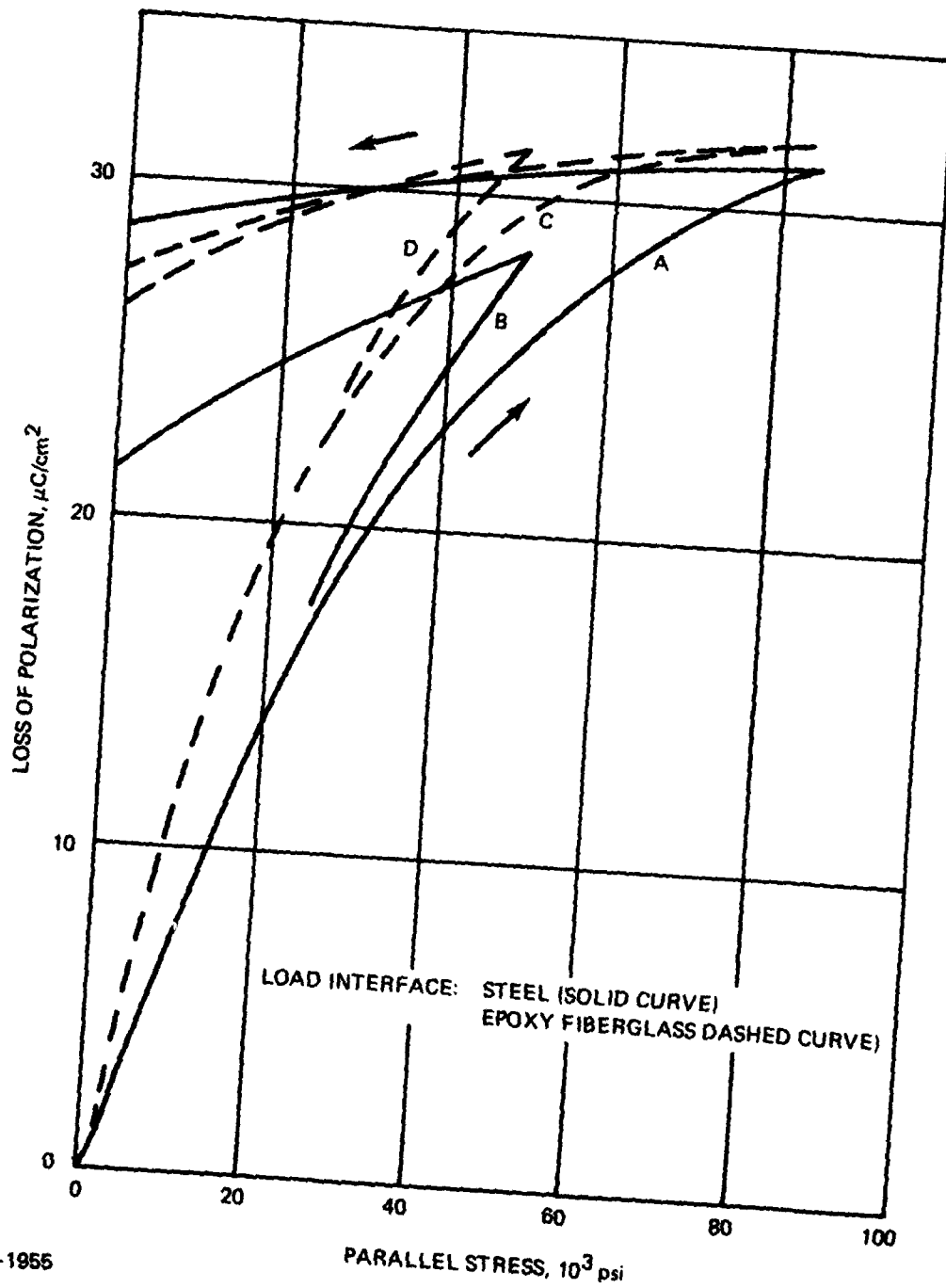
$$A = \text{test specimen area, cm}^2$$

Figure 16 presents PZT-5A test specimen output using the 2.02 μF capacitor. Curve A represents the output using hardened steel loading blocks directly in contact with the test specimen surfaces. The peak stress applied for curve A is 425,000 kg/m^2 (85,000 psi) with P_r of 29 $\mu\text{C}/\text{cm}^2$. After stress removal P_r reduces to 26 $\mu\text{C}/\text{cm}^2$. Curve A represents the average of four specimen tests. The extreme values measured during the tests are represented by the limits of the vertical bars shown. The remanent polarization for PZT-5A is 38 $\mu\text{C}/\text{cm}^2$. This output was not attained due to edge effects and the



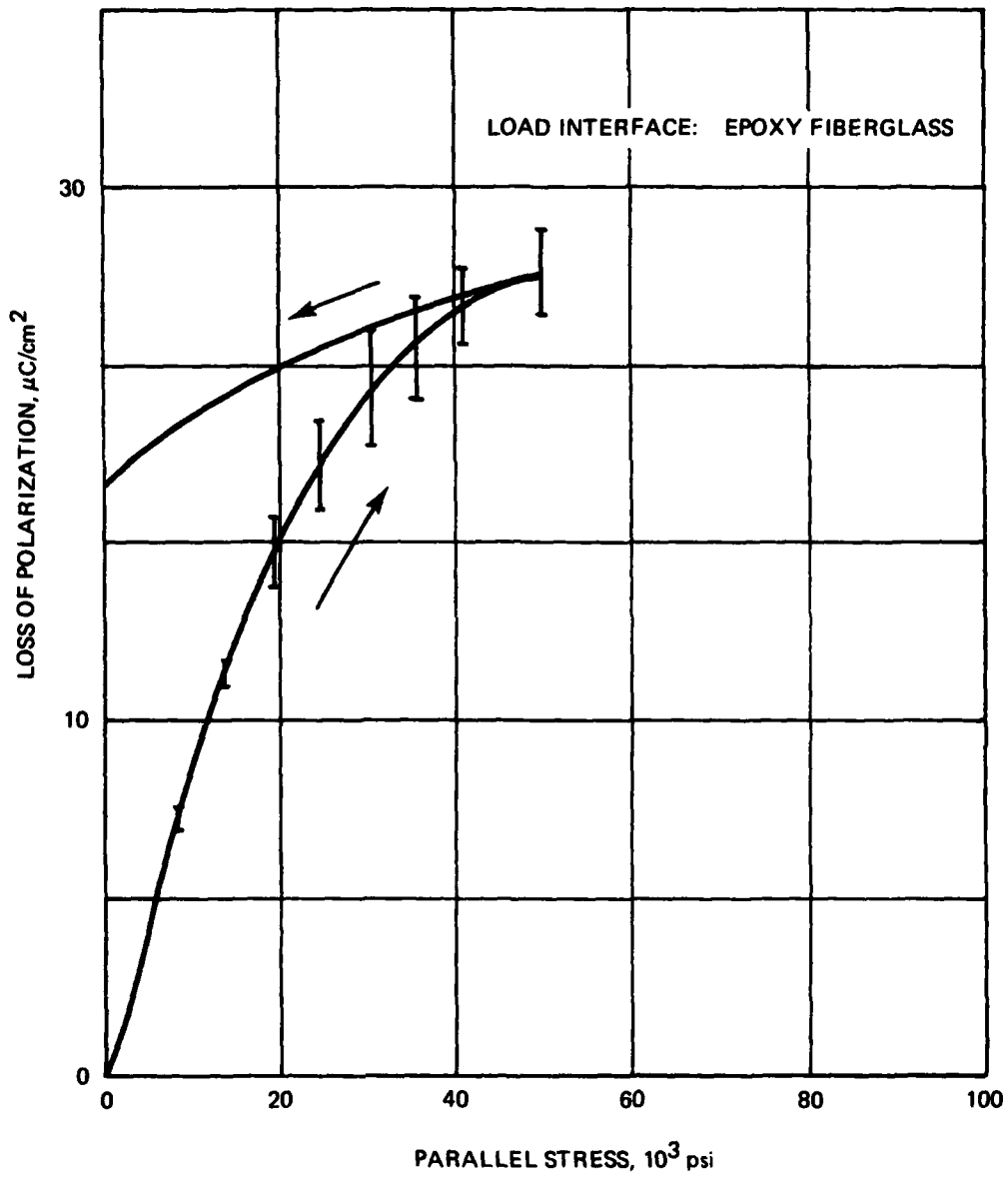
99-1954

FIGURE 16. LOSS OF POLARIZATION OF PZT-5A through 2.02 μF MYLAR CAPACITOR.



99-1955

FIGURE 17. LOSS OF POLARIZATION OF PZT-5A THROUGH 0.0483 μF MYLAR CAPACITOR.



99-1956

FIGURE 18. LOSS OF POLARIZATION OF PZT-5A THROUGH 0.0308 μF MYLAR CAPACITOR.

fact that applied stress must exceed $425,000 \text{ kg/m}^2$ (85,000 psi) for more complete depolarization under the mounting conditions used.

Curve B of figure 16 represents the average output for two specimens stressed to $250,000 \text{ kg/m}^2$ (50,000 psi) using the same steel loading blocks used to obtain curve A. Curve B shows that P_r is $24 \text{ } \mu\text{C/cm}^2$ at $250,000 \text{ kg/m}^2$ (50,000 psi) and is $19 \text{ } \mu\text{C/cm}^2$ after stress removal.

Curve C (one test specimen) of figure 16 was obtained under conditions similar to curve B except that copper-clad epoxy fiberglass laminate pads 0.035 cm (0.014 in) thick were placed between the test specimen and the load blocks. Curve C indicates P_r is $26.5 \text{ } \mu\text{C/cm}^2$ at $250,000 \text{ kg/m}^2$ and reduces to $23.5 \text{ } \mu\text{C/cm}^2$ following stress removal. Comparing curves B and C, it is seen that a significant improvement in output is produced when the pads are used. This is attributed to a more uniform stress distribution and increased radial compliance at the piezoid interface resulting from the presence of the pads.

The output performance of PZT-5A test specimens with an external capacitance of $0.0483 \text{ } \mu\text{F}$ was measured and recorded (fig. 14). Curves A (two test specimens) and B (three test specimens) were obtained with direct contact between the test specimen and the steel load blocks. Curves C (one test specimen) and D (three test specimens) were obtained using the same type of epoxy fiberglass laminate pads that were used to generate curve C in figure 16. Again, it had been noted that performance was improved when the pads are added. Comparing curves B and D in figure 4, the output after stress removal was increased from $21.5 \text{ } \mu\text{C/cm}^2$ to $26 \text{ } \mu\text{C/cm}^2$ with the addition of the pads.

It was also observed that there was greater percentage decrease in P_r from peak stress to the unstressed state for the cases where the $0.0483 \text{ } \mu\text{F}$ capacitor was used (fig. 17) in comparison to the comparable cases where the $2.02 \text{ } \mu\text{F}$ capacitor was used (fig. 16). This occurred because the higher voltage gradient generated across the piezoid when the low capacitance load was present tended to inhibit depolarization.

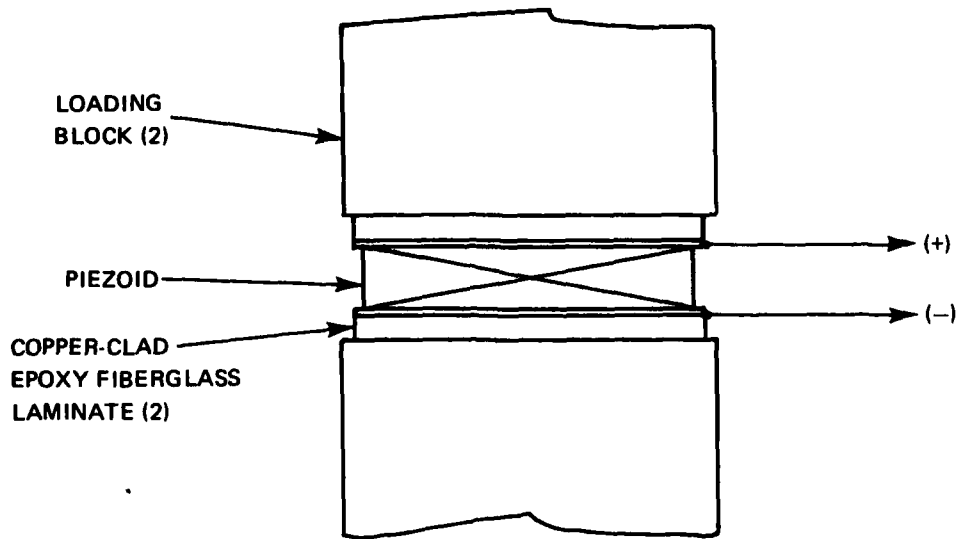
The output performance of two PZT-5A specimens tested with the $.0308 \text{ } \mu\text{F}$ capacitor were recorded in figure 18. The epoxy fiberglass laminate pads were included in these tests. Average P_r after stress removal was $16.5 \text{ } \mu\text{C/cm}^2$. Comparing the depolarization

curve of figure 18 with curve D in figure 17 indicated that less charge was released when the 0.0308 μF ceramic capacitor was used. Since the voltage gradients did not differ significantly between the two cases, the performance variation was attributed to the capacitors used. The 0.0483 μF capacitor had a stable, low-loss, mylar dielectric material. The 0.0308 μF capacitor had a ferroelectric ceramic dielectric material. It was assumed that the reduced charge stored was related to polarization phenomena within this dielectric material. Although this difference in performance was noted, the ceramic capacitor remained as the choice for the fuzing system because of its physical ruggedness and small size.

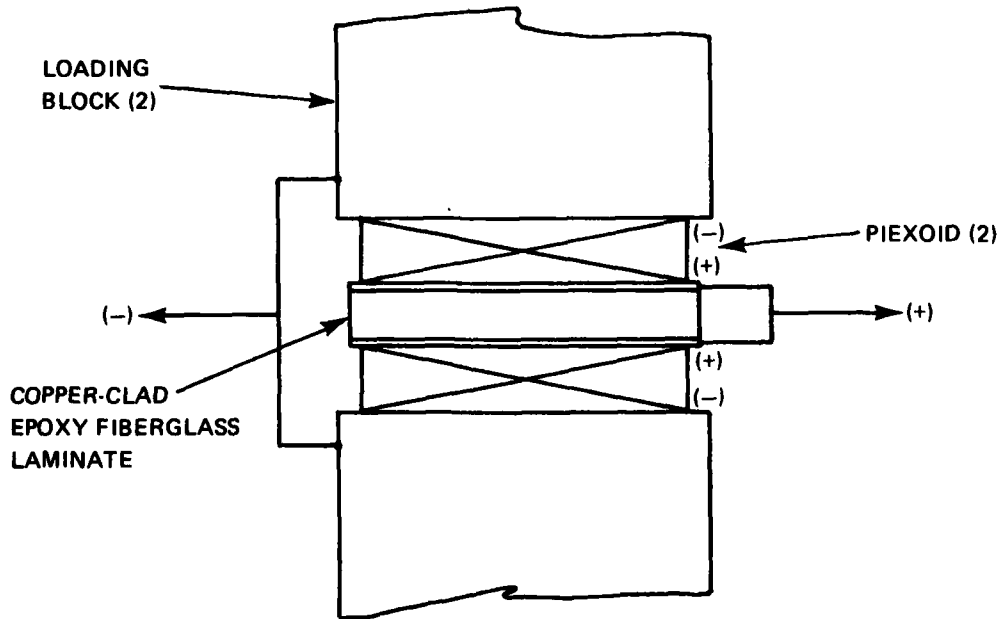
In the fuze concept, the energy stored in the capacitor must be sufficient to fire a microdetonator having a bridgewire resistance of 4.0 to 9.0 ohms and which has a standard all-fire specification of 300 microseconds maximum function time when initiated by a 100 μF source charged to 1.6 volts. The maximum time constant for the quoted condition is $(100 \mu\text{F}) (9.0 \text{ ohms}) = 900$ microseconds, therefore, in 300 microseconds it can be shown that 51% of the stored energy is transferred to the load. The stored energy was computed as 1280 ergs. The energy transferred within 300 microseconds was then 653 ergs and represented the all-fire energy under the specified test conditions. The circuit time constant in the fuzing system will be less than one microsecond and, since the all-fire energy tends to reduce as the power is increased, 653 ergs represent a conservative all-fire energy specification.

The loss of polarization for piezoids tested using the 0.0308 μF capacitor is presented in figure 15. Additional information for these piezoid is contained in table 6, tests number 1 and 2. This table lists the voltage, loss of polarization, and energy stored in the external capacitor for the states of 250,000 kg/m^2 (50,000 psi) peak stress and stress removal. The test configuration represented by tests 1 and 2 is designated as configuration "A" in table 6. This refers to the single-piezoid arrangement, shown in figure 19a, containing the epoxy fiberglass laminate pads at the load block interfaces.

A dual-piezoid arrangement, designated as configuration "B" in table 6, was also tested. This consisted of a copper-clad epoxy fiberglass laminate with a thickness of 0.071 cm (0.028 in) placed between two piezoids stacked and wired to be electrically in parallel. The outer surfaces of the piezoid stack were placed directly in contact with the steel load blocks. This configuration is illustrated in figure 19b. Test results are presented in table 6, tests number 3 and 4.



CONFIGURATION "A"



CONFIGURATION "B"

99-1957

FIGURE 19. PIEZOID TEST CONFIGURATIONS.

Table 6. Test results (single - and dual - piezoid energy generator configurations) of quasi-static tests

Test No.	Piezoid Configuration	Output at Peak Stress of 250,000 kg/m ²			Output After Stress Removal		
		Voltage (volts)	Loss of Polarization ($\mu\text{C}/\text{cm}^2$)	Energy Stored in External Capacitor (ergs)	Voltage (volts)	Loss of Polarization ($\mu\text{C}/\text{cm}^2$)	Energy Stored in External Capacitor (ergs)
1	Single ("A")	123	21.4	2330	89	15.5	1220
2	Single ("A")	137	23.8	2890	102	17.7	1600
3	Dual ("B")	240	20.9	8870	150	13.0	3460
4	Dual ("B")	270	23.5	11230	170	14.8	4450

- Notes: 1. Ferroelectric material: PZT-5A
 2. External capacitor: .0308 μF ceramic

The data in table 6 indicates that the single-piezoid configuration, stressed to a peak of 250,000 kg/m² resulted in residual energy outputs of 1220 ergs and 1600 ergs for the two specimens tested. These energy values are about twice the required all-fire energy. The dual-piezoid configuration provided energy in excess of five times the required all-fire energy. Since the dual-piezoid approach provided a significant safety margin for a small penalty in volume, it was selected as the reference design and was implemented for gun tests.

Two specimens of PSZT 80/20-5-2 Nb with a characteristic remanent polarization of 35 $\mu\text{C}/\text{cm}^2$ were tested using the 0.0483 μF capacitor. Each specimen was mounted as shown in figure 16a. At 235,000 kg/m² (47,000 psi) the loss of polarization averaged 29 $\mu\text{C}/\text{cm}^2$. This result was not significantly different than results obtained for PZT-5A tested under similar condition. The particular PSZT specimens tested fractured at 250,000 kg/m². In these tests, the benefit of this PSZT material was not apparent under the loading conditions selected to simulate a near-term application. Under hydrostatic stress conditions this composition depolarizes at 100,000 kg/m² however, under the one-dimensional strain condition which was approached in the configuration tested, loss of polarization versus stress is approximately the same as PZT-5A. It was concluded that PZT-5A was the better material because it is more stable (Curie temperature of 360°C versus 150°C for PSZT) and has a much more extensive application history.

The dynamic tests were conducted to gain some insight into regarding depolarization when the depoling stress is maintained for brief periods only. The test setup of figure 15 was used. The piezoid mounting arrangement corresponded to that of figure 19a and the 0.0308 μF capacitor was used. The stress pulse generated has an approximate half-sine waveform. One test specimen was exposed to a stress pulse of 0.5 millisecond duration with a peak stress of 300,000 kg/m². The pulse remained above 250,000 kg/m² for 0.1 millisecond. The output voltage was 85 volts immediately after pulse application and drifted to 77 volts in approximately one minute and maintained this value. A second test applied a peak stress of 350,000 kg/m² to a test specimen. The pulse remained above 250,000 kg/m² for 0.15 millisecond. Test specimen output was 80 volts immediately after pulse application and drifted to 75 volts, behaving in a manner similar to the first specimen. In quasi-static testing to 250,000 kg/m², test specimens produced an average of 95 volts (tests number 1 and 2 of table 6). In dynamic testing where stress levels exceeded 250,000 kg/m² for up to 0.15 millisecond

the average stabilized output was 76 volts. This is 80 percent of quasi-static results. The conclusion drawn from this experiment was that output performance based on quasi-static testing should be derated in predicting ballistic performance. Some conservatism was contained in the dynamic tests since a representative 30MM setback profile has a pulse duration of 2.5 milliseconds rather than the 0.5 millisecond duration of the conducted tests.

Gun Tests

Purpose of Tests

Analysis and laboratory tests clearly indicated that the reference projectile fuze system which depolarized a piezoid during setback, charged a capacitor and initiated a detonator on impact with the target was feasible with present state-of-the-art components. Gun tests were planned and conducted to test the fuze concept in a 30MM projectile and to obtain a measure of the fuze response. The primary purpose of the tests was to determine that the fuze did not function during the gun environment and that it functioned properly upon impact against targets at normal and graze impacts.

Test Projectiles

The 30MM test projectiles were fabricated from WECOM 30 parts which were provided as government furnished parts. These parts were a projectile body with an internal 0.960 - 32 NS thread at the ogive, an aluminum disc with matching threads, and an aluminum nose cap (part number 8889445). Each of these parts was modified to house the gun test assembly. The body was machined internally to an exact inside diameter and externally with a crimp groove to attach the nose cap. The disc was machined for a locking nut to hold the test assembly in the body. The nose cap was stripped of the anodized finish so it could be used as one side of a deformation impact switch.

The 3010 grain test projectile and all its parts is shown in figure 20.

The fuze assembly was made up of three modules, each having a specific function. The aft module consisted of the pair of PZT-5A piezoids, a common conductor between them, a tungsten mass, a steel anvil and a two piece housing. The center module contained the capacitor, the detonator and the electrical connections between them in another two piece housing. The forward module was

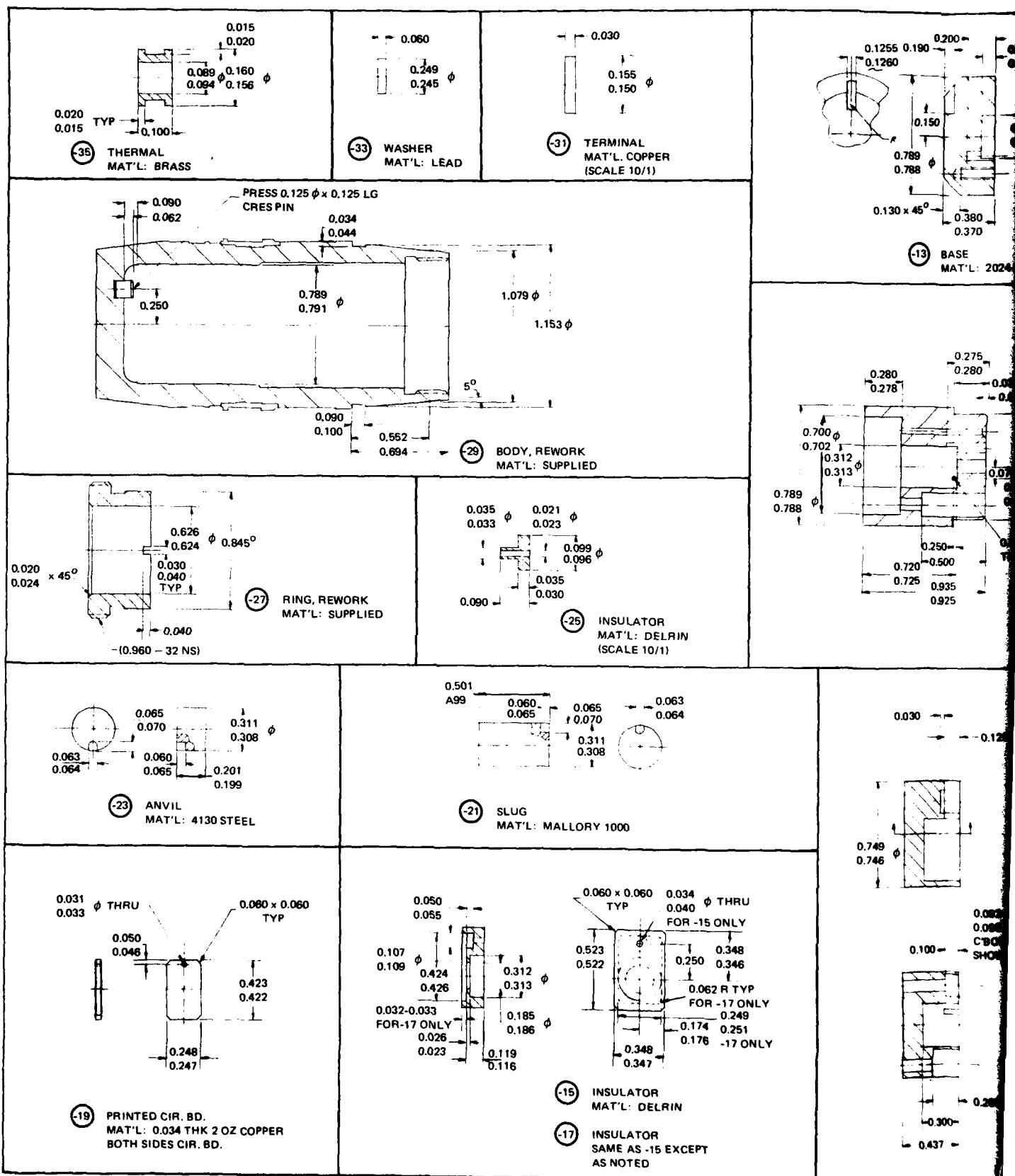
22

21

A/R			POTTING COMP.				28
A/R			WIRE				27
3		0.086 -56 x 0.50 LG	SHCS				26
2		0.086-56 x 0.50 LG	PAN HD SCREW	BRASS			25
1		0.112-40 x 18 LG	SET SCREW				24
2		0.062 DIA x 0.12 LG	DOWEL PIN				23
2		0.062 DIZ x 0.38 LG	DOWEL PIN				22
1			CAP				21
2		06401-1					20
1	19113	06401-1	MICRODETONATOR				19
1			OGIVE	SUPPLIED			18
1		-35	TERMINAL				17
1		-33	WASHER				16
1		-31	TERMINAL				15
1		-29	BODY				14
1		-27	RING				13
1		-25	INSULATOR				12
1		-23	ANVIL				11
1		-21	SLUG				10
1		-19	PRINTED CIR. BD				9
1		-17	INSULATOR				8
1		-15	INSULATOR				7
1		-13	BASE				6
1		-11	HOUSING				5
1		-9	INSULATOR				4
1		-7	HOLDER				3
1		-5	HOUSING				2
1		-3	INSULATOR				1
QTY REQD	CODE IDENT	PART OR IDENTIFYING NO.	NOMENCLATURE OR DESCRIPTION	MATERIAL OR NOTE	SPECIFICATION	ZONE	ITEM NO.

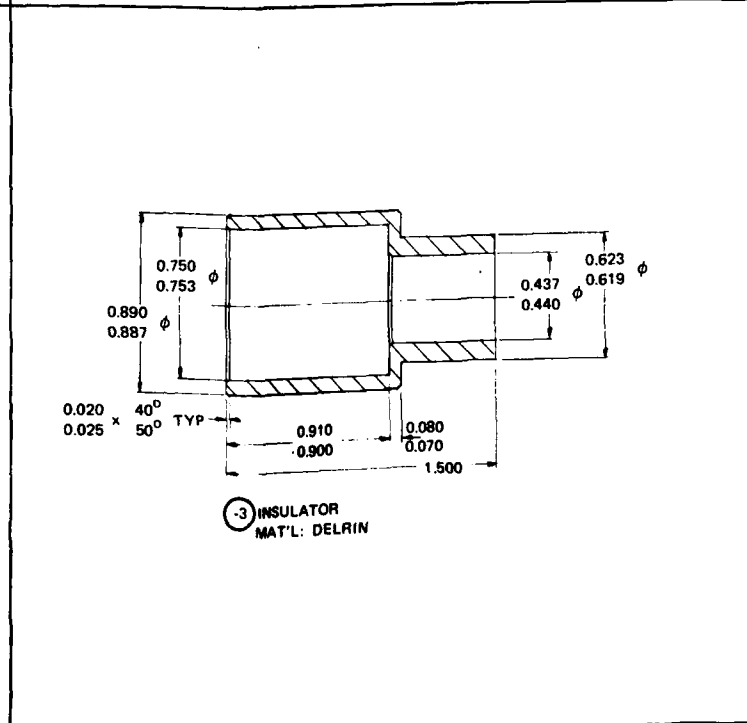
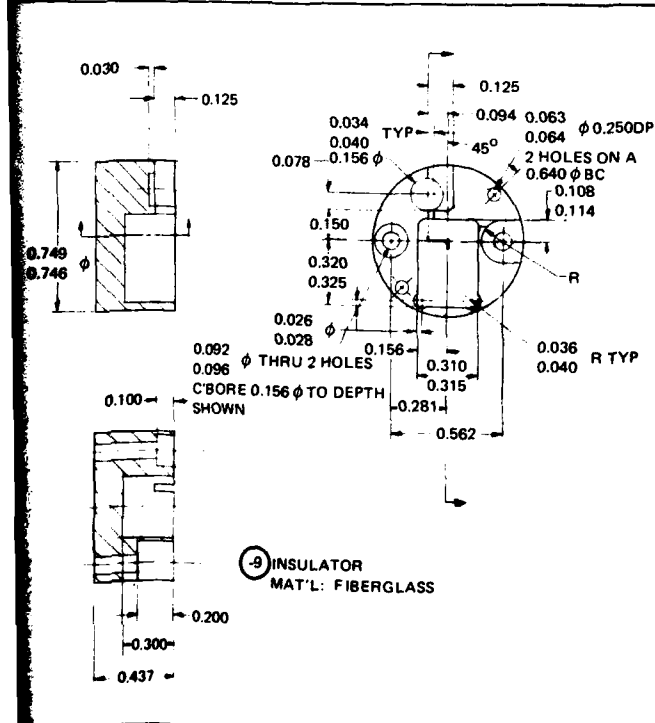
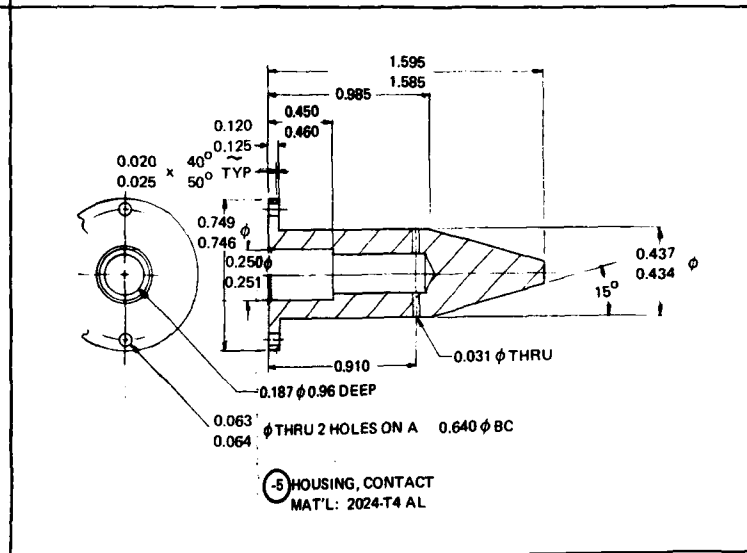
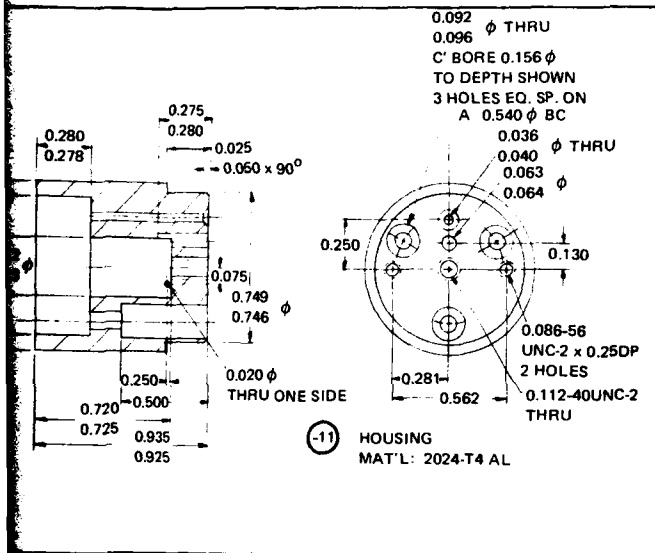
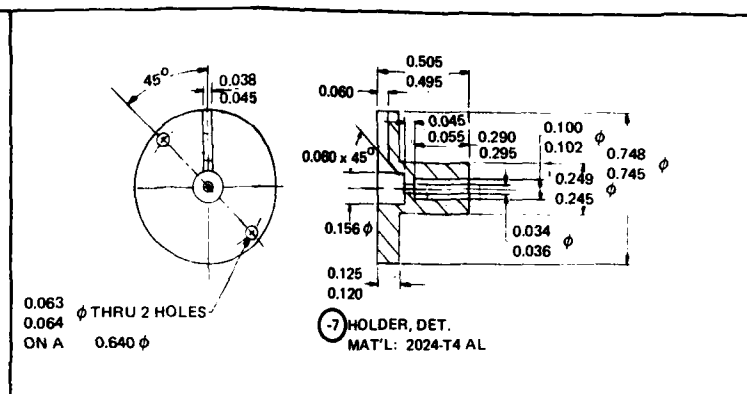
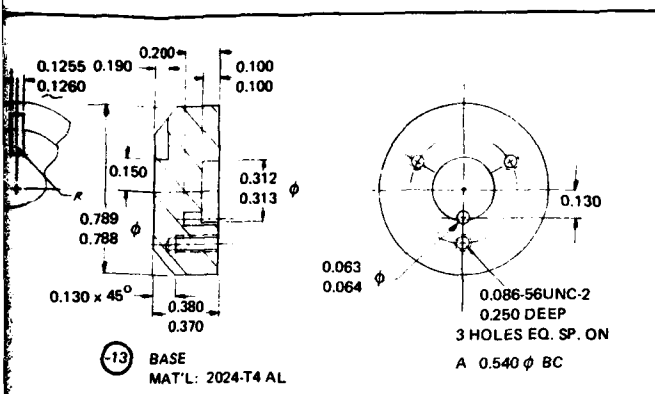
BASE FUZE TEST PROJECTILE.

2



99-1958

FIGURE 20B. 30MM BASE FUZE T



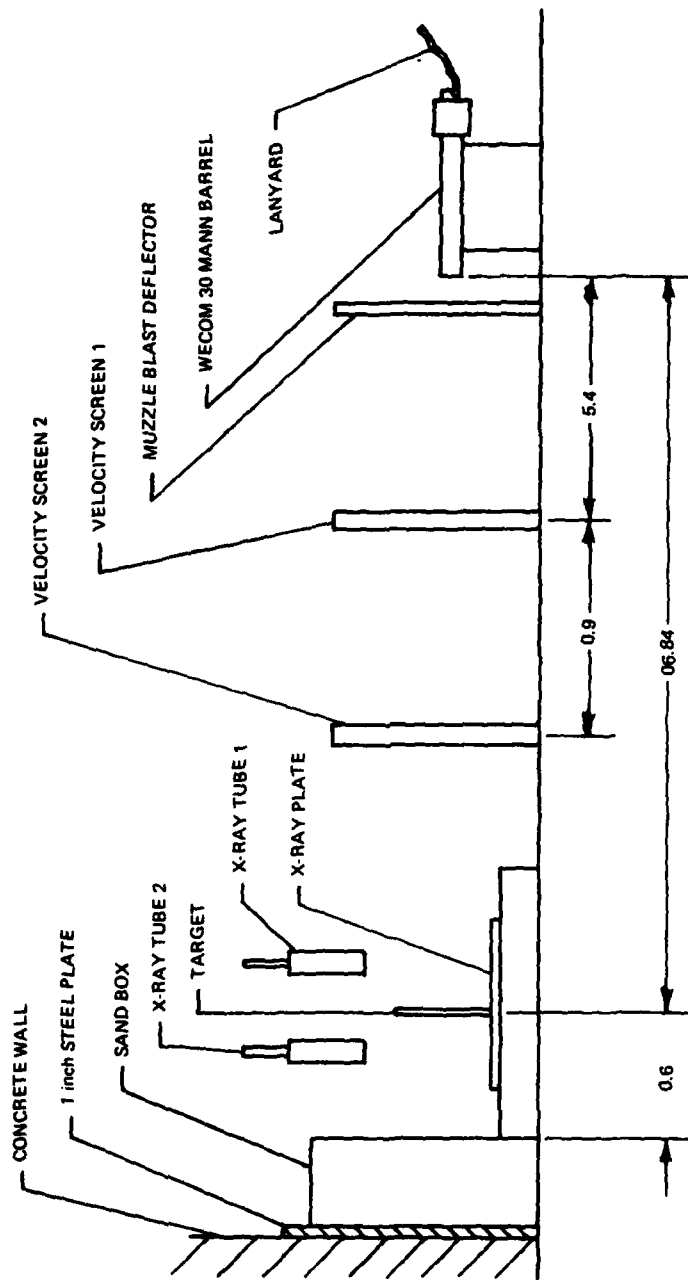
an aluminum probe that was the other side of the deformation switch and that had an internal cavity for venting the gases from the detonator. A lead disc between the detonator and the internal cavity was included to serve as a witness that the detonator fired.

Calibration Tests

Gun tests were conducted to calibrate the propellant charge needed to achieve impact velocity of 600 m/sec. Test projectiles were attached to WECOM 30 cartridge cases which were charged with X3337.7 propellant which is a rolled ball propellant manufactured by Olin Corporation. This propellant has recently been designated WC 858. The projectiles were bonded into the cartridge cases with Eastman 910 adhesive. This band and the interference fit between projectile and case prevented the projectile from becoming loose during handling and transportation after assembly. Nine calibration tests were conducted with WECOM 30 target practice projectiles and a WECOM 30 Mann Barrel. A summary of the tests is in table 7. Pressure readings were measured a piezoelectric transducer, PCB 1199 with a sensitivity of 0.828 pc per kg/m^2 (0.140 pc/psi). Since the test projectiles with fuzes was expected to weigh approximately 207 grams, it was decided to use a charge of 45 grams of X3337.7 propellant in the fuze function tests.

Projectile Tests

The test setup for the gun tests to observe fuze performance is shown in figure 21. The WECOM 30 Mann Barrel was mounted on a test bed 6.84 meters from the target plate. A lanyard attached to the hammer on the breech assembly was used to fire the gun from a remote station. A muzzle blast suppressor was used to protect the instrumentation. A pair of velocity screens were mounted 5.4 meters from the muzzle and 0.9 meters apart. The second velocity screen was used to trigger the 300 KEV flash x-ray equipment for the first x-ray picture. Two x-ray tubes were suspended over the target plate; the first to view the projectile before impact and the second to view the projectile after impact. The first picture was to ascertain that the fuze was intact and did not pre-fire due to the gun firing environment. The second picture activated by a foil switch on the target was to show that the detonator fired. Since the only power in the projectile was that generated during setback, the fired detonator would demonstrate that the fuzing system performed as designed. The target plate was 30 x 30cm (1 x 1 ft) sheet of 2024 - T4 aluminum. For normal impact tests, the thickness was 0.229 cm (0.090 in). For the graze impact



99-1969

FIGURE 21. SETUP FOR GUN TESTS.

Table 7. Propellant calibration

Test No.	Projectile	Propellant	Peak	Velocity	Remarks
	Weight	Charge	Pressure		
	Grams	Grams	Kg/m ²	M/sec	
Cal 1	195	45	- a -	-	
2	195	45	- a -	-	
3	195	45	137,000	638.4	Changed velocity screen sensitivity Hit screen
4	195	45	151,000	-	
5	195	45	138,000	642.3	
6	195	40	- a -	576	
7	195	40	106,500	579.6	
8	195	35	- b -	551.7	
9	195	35	86,000	513.9	

a. Firing delay too long to read pressure.

b. Firing delay too short to read pressure.

test, the thickness was .16 cm (0.063 in) so that the in-line target thickness was constant for all tests. Behind the target, a sand box backed up with a steel plate and a concrete wall was used to capture the projectile.

Six gun tests were conducted with excellent results in each test. A seventh test (test number 3) was a no test because a faulty operation of the flash x-ray equipment. A summary of the gun tests is in table 8. All tests were conducted between November 4, 1978 and November 10, 1978. The x-ray film was processed at Avco's Non-Destructive Test Laboratory.

The first test was conducted with a normal impact. The second x-ray was taken 155 microseconds after impact. The x-ray picture for test one is shown in figure 22. Before target impact, the lead azide pellet in the detonator was intact and the cavity behind the lead disc was clear. After impact, the lead azide pellet is gone and the cavity has debris from the lead disc. These pictures demonstrated that the detonator was not detonated prior to impact, but it had fired within 155 microseconds after impact.

The second test conducted in the same manner as test one showed the same results. Figure 23 is the x-ray picture.

Test number three had a malfunction in the x-ray equipment, resulting in no pictures during the test. This was a no test since no conclusions could be made.

The fourth test was similar to test number one except the second x-ray was taken 50 microseconds after target impact. Time was reduced to get a better measure of fuze response. The second x-ray (fig. 24) clearly showed that the detonator had fired within 50 microseconds after impact.

For the fifth test, the target plate was tilted to an angle of 45 degrees and in order to avoid additional thickness in-line ahead of the projectile, an 0.16 cm. aluminum plate was used for the test. The second x-ray taken 50 microseconds after impact (fig. 25) showed that the detonator had fired. For this and subsequent tests, the first x-ray tube was removed from the test setup since it had been verified during previous tests that the detonator and the fuzing elements were unaffected by the gun environment.

Table 8. Gun test data

Test No.	Target Thick Centimeter	Graze Angle Degree	Velocity m/sec	Time Between		Time After Impact	Detonator	Remarks
				Pictures	Microsec.			
1	.229	90	628.5	271	155	Fired		
2	.229	90	626.7	279	155	Fired	(a)	
3	No Test							
4	.229	90	646.5	138.1	50	Fired		
5	.16	45	655.5	-	50	Fired	(b)	
6	.16	45	645.6	-	25	Fired	(b)	
7	.229	90	658.8	-	25	Fired	(b)	

(a) Tube #1 pre-triggered twice over-exposing the film

(b) Removed Tube #1

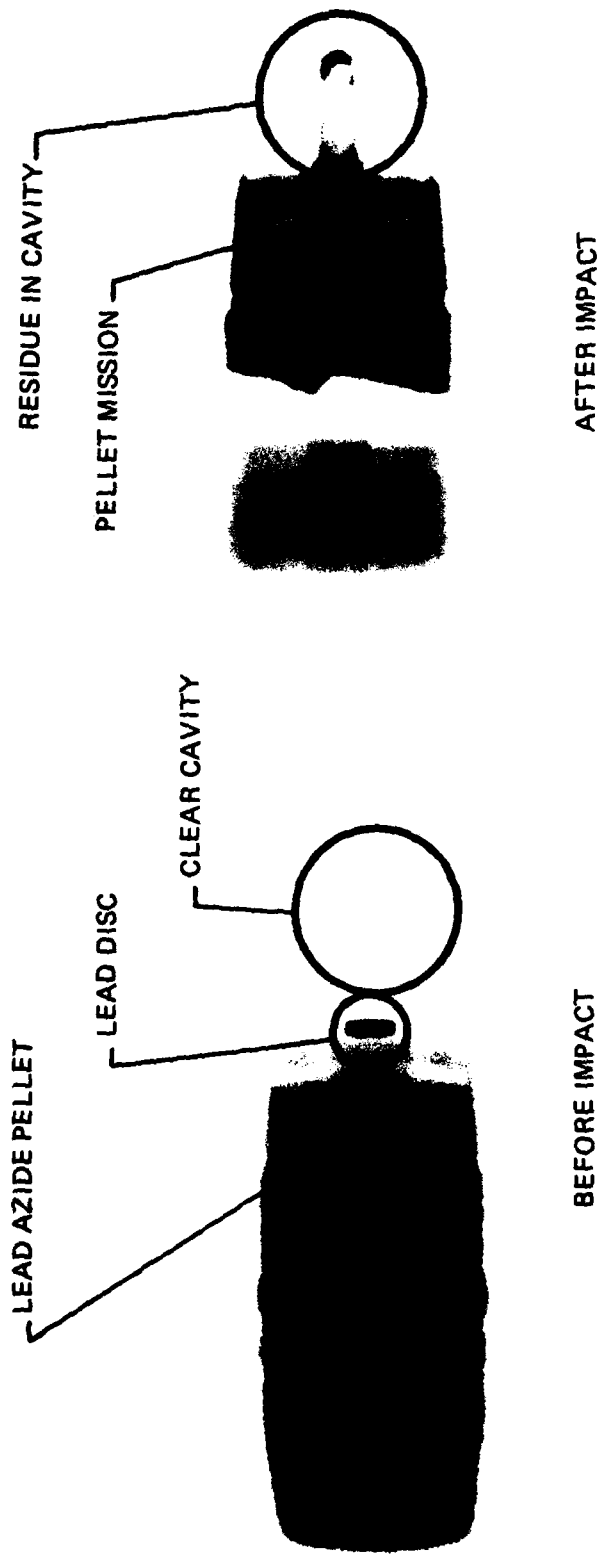
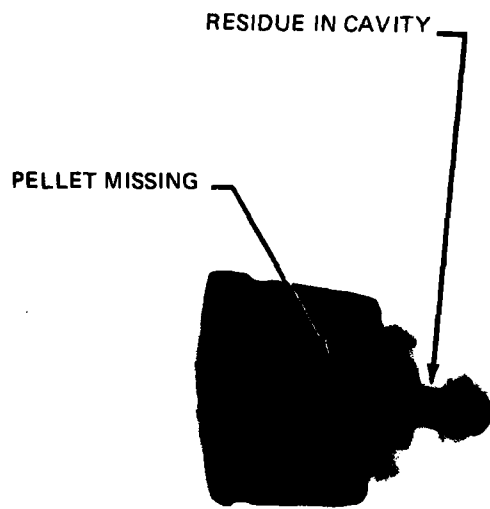


FIGURE 22. X-RAY PICTURE OF TEST 1.

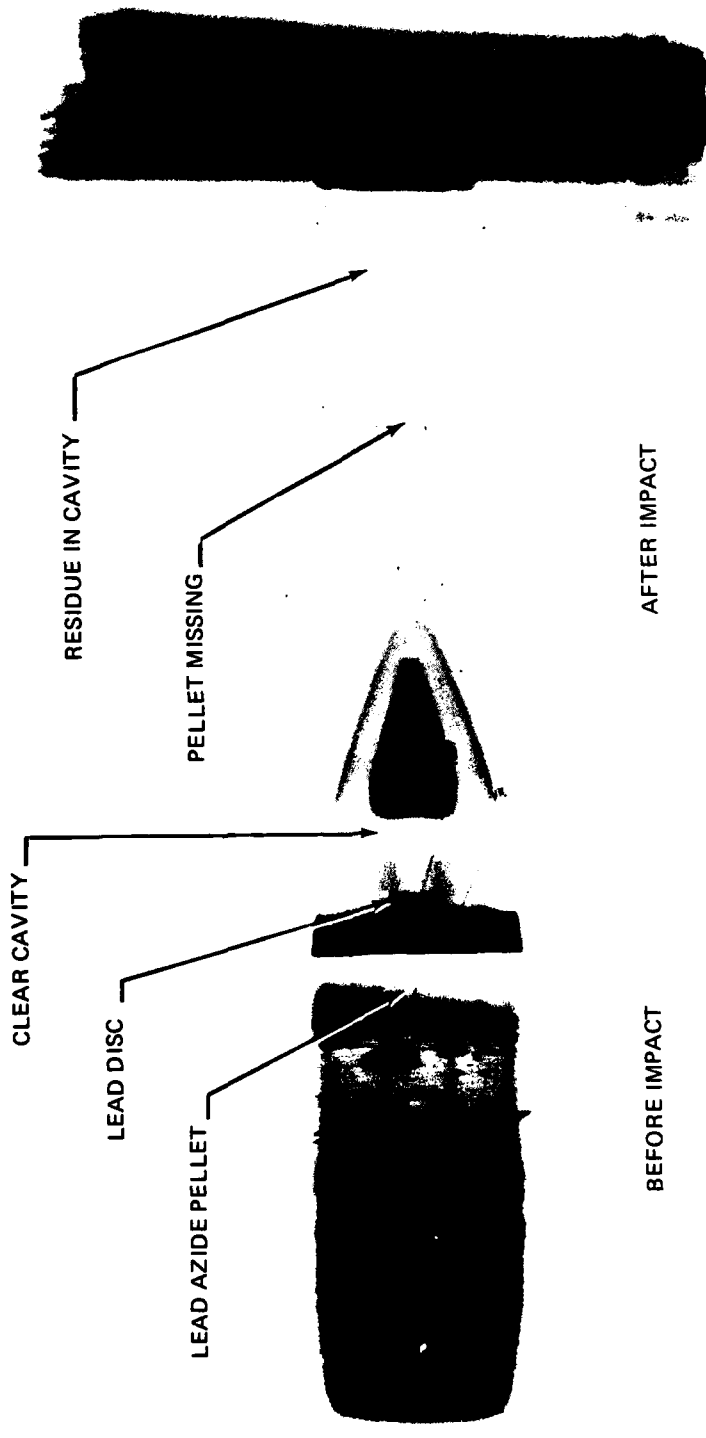
99-1960



AFTER IMPACT

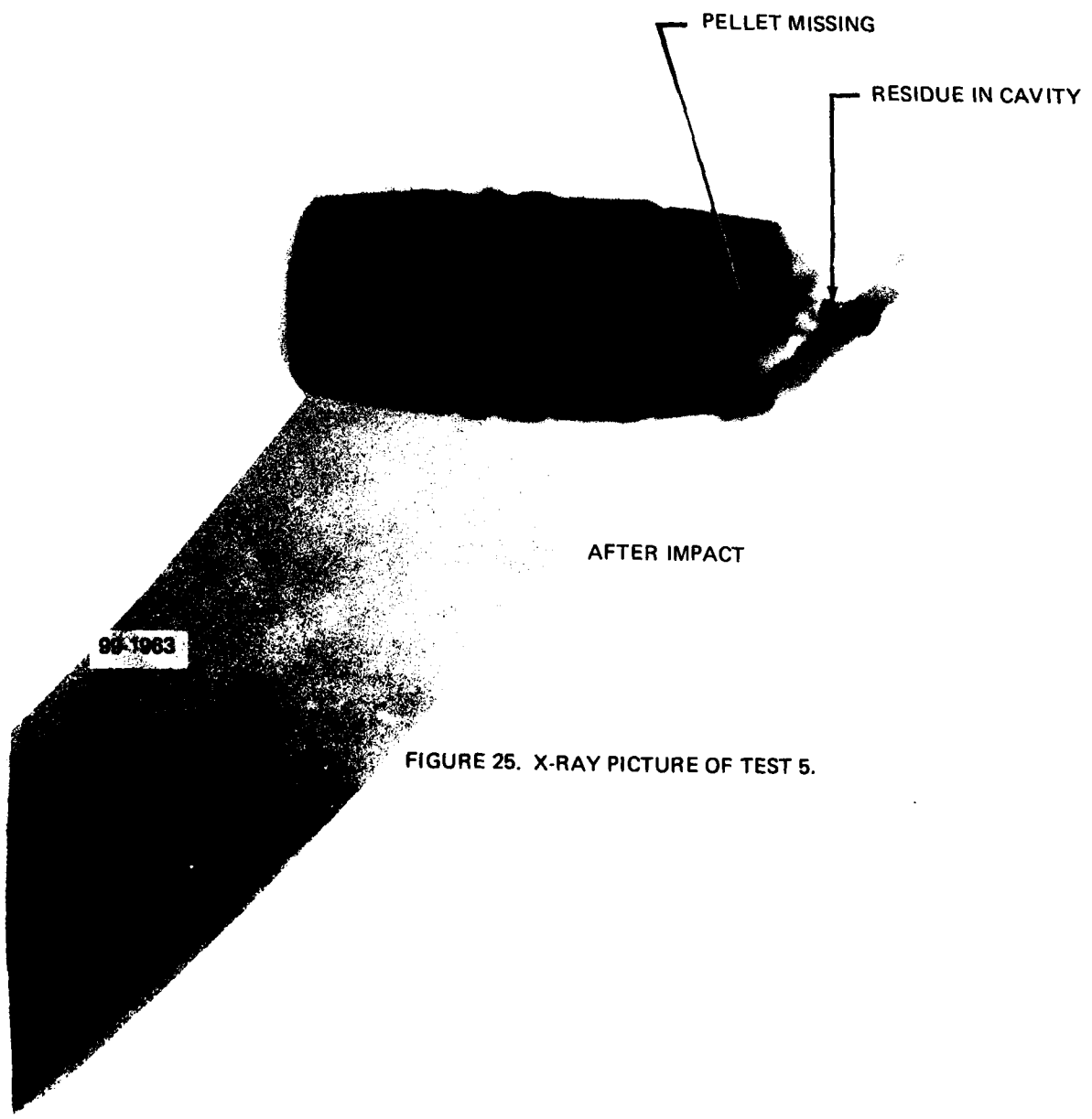
99-1961

FIGURE 23. X-RAY PICTURE OF TEST 2.



99-1962

FIGURE 24. X-RAY PICTURE OF TEST 4.

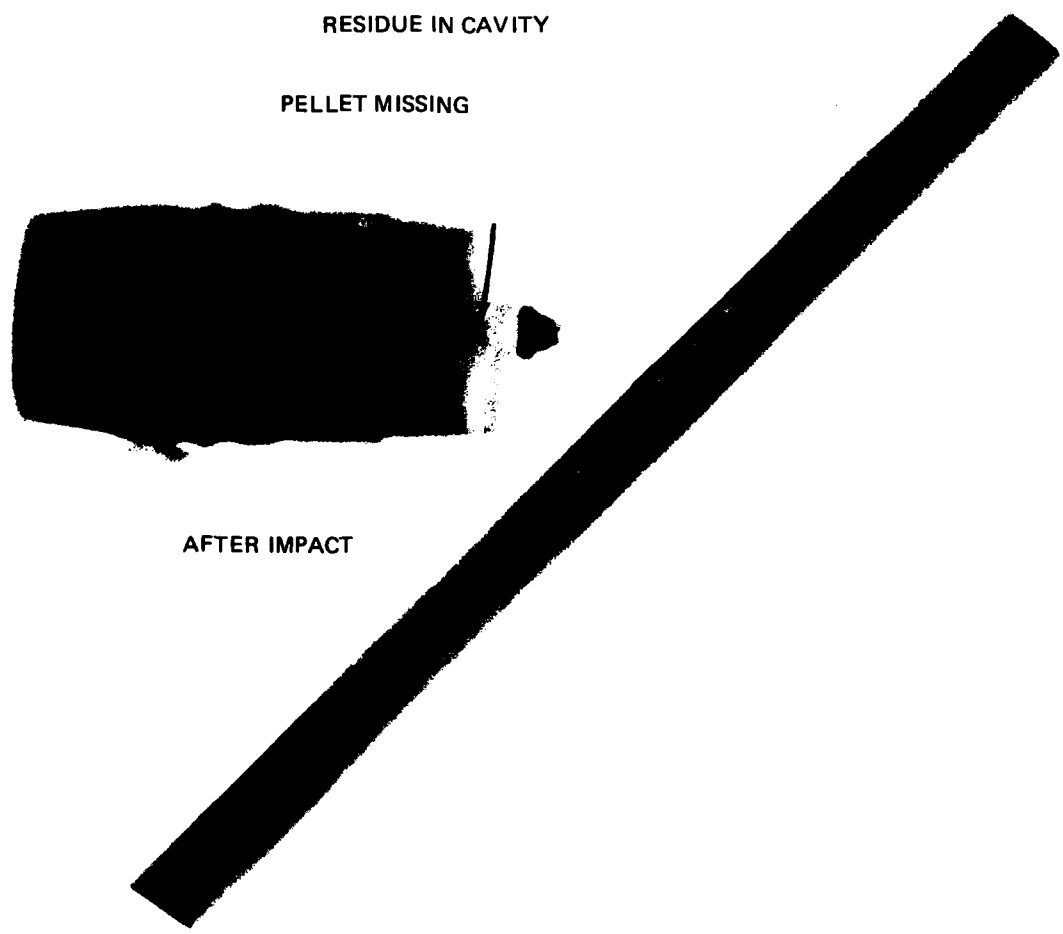


AFTER IMPACT

FIGURE 25. X-RAY PICTURE OF TEST 5.

Test number six was similar to test number five, but the time of the x-ray was reduced to 25 microseconds after impact. The picture in figure 26 shows that the lead disc behind the detonator has just begun to breakup. This picture indicated that the fuze response was just under 25 microseconds for the conditions of the test.

The seventh and last test was a repeat of test number one with the x-ray picture taken 25 microseconds after impact. The picture in figure 27 showed the same results as test number six. The lead disc is beginning to break up, indicating that the fuze response was just under 25 microseconds.



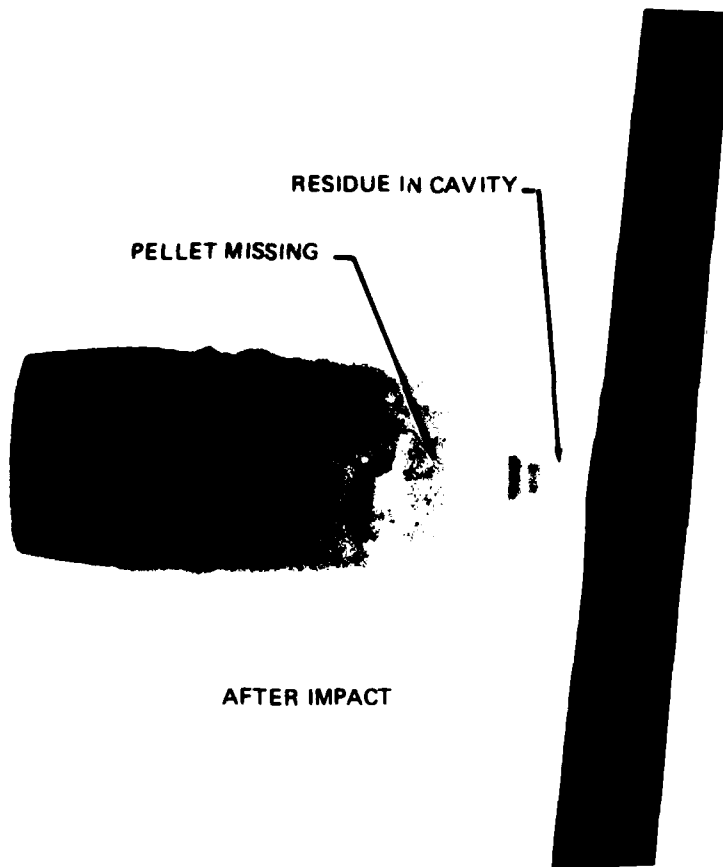
RESIDUE IN CAVITY

PELLET MISSING

AFTER IMPACT

99-1964

FIGURE 26. X-RAY PICTURE OF TEST 6.



RESIDUE IN CAVITY

PELLET MISSING

AFTER IMPACT

99-1965

FIGURE 27. X-RAY PICTURE OF TEST 7.

RELIABILITY
(CDRL Item A005)

A preliminary reliability assessment was made of the base fuze design using piecepart data of the four elements of the fuze, ferroelectric crystal, ceramic capacitor, mechanical crush switch and microdetonator. A reliability of 0.9988 was calculated for the fuze circuit.

The reliability for the pair of ferroelectric crystals was 0.9999. This was found by using a conservative reliability of one crystal (R_{X1}) as 0.99. Since ($R_X = R_{X1}$), the combination computed to 0.9999. Until more data is accumulated, it was assumed that sufficient energy is generated during setback from one crystal to fully charge the capacitor. The load on the crystal and the exposed area of the crystal influence the crystal output. These factors will have to be kept in mind during the integrated design of the safing and arming elements with the fuze components.

Reliability of the ceramic capacitor was based on the fact that the same capacitors have been used by Harry Diamond Laboratory during numerous tests in gun environments as high as 30,000 g's without any failures. Published data for ceramic capacitors at a temperature of 100°C and at 50 percent efficiency determined a reliability factor greater than 0.999999.

The crush switch reliability was assessed at 0.9999. Upon impact with the target, the two plates will come together and make contact. The reliability was determined to be that of the connections from the switch to the other parts of the fuze circuit. The limiting elements was assumed to be the solder connections which traditionally have a reliability of 0.9999.

Reliability of a single wire bridge microdetonator was given 0.999 at 95 percent confidence. This value was consistent to that used during a previous design study for a mortar fuze using a very similar device. The microdetonator reliability was the limiting value to the overall fuze system reliability. Since the four fuze elements function in series, the preliminary system reliability was the product of the reliabilities as presently assigned.

HAZARD ANALYSIS
(CDRL Item A006)

The microdetonator was the only explosive element in the base fuze concept. A determination of the potential hazard of the test projectiles with the microdetonator was made with a static test and later supplemented with a gun test.

A static test was made with a fully assembled test projectile that had a hole in the base of the body for passage of wires to the detonator from an exterior power source. The projectile was placed in a metal box in an evacuated room. The detonator was fired and the projectile examined in detail for damage or fracture. The outward appearance of the projectile did not indicate anything unusual. The nose cap was still attached and there was no expansion of the projectile body. All interior components were intact and the only noticeable effect was a slight bulge in the walls of the detonator housing (number 3 of figure 20).

It was observed in the first gun tests that the target plates were peeled back, but the target plates of the calibration tests had clean circular holes. It was suspected that the peeling was caused by the explosion of the detonator. During the static safety test the internal pressure after detonation may have been relieved through the hole in the projectile base and did not blow off the nose cap. During the gun test, this pressure may have caused the peeling effect on the target plate. Although the x-ray pictures did not show this effect, it was possible that it occurred after 155 microseconds.

The series of gun tests was interrupted in order to fire a projectile without a detonator into a target plate. Since test projectiles were scarce, the same projectile used in the static test was used for this purpose. The hole in the base of the body was plugged with a tight fitting machine screw. The projectile was assembled to a cartridge case charged with 45 grams of X3337.7 propellant and fired in the same manner as the test projectile of the gun tests. The hole in the 0.229 cm thick target plate had the same peeling effect as the test projectiles.

It was concluded that the difference in the holes made in the target plates was caused by the configurations of the projectiles. For the calibration shots, the projectiles P/N 9252416 had a hollow ogive and at impact, the aluminum nose cap collapsed and the projectile body P/N 9252418, cut through the target like a cookie cutter, leaving a clean round hole. The base fuze test projectiles had a housing in the

ogive for the impact switch/sec (fig. 20). The point on the housing pierced the target and as the projectile passed through the target, the aluminum "peeled" back away from the impact point.

It was further concluded that test projectile for the base fuze experiments does not present any hazards and it is safe to handle.

CONCLUSIONS AND RECOMMENDATIONS

Conclusions

The following general conclusions were reached on the basis of analysis, laboratory tests and test firings:

1. The most feasible base fuze design uses a point initiating impact sensor, an energy generator activated at setback, a storage capacitor, and a microdetonator.
2. A dual piezoid arrangement using PZT-5A ferroelectric ceramic crystals provides sufficient energy to fire a microdetonator under all anticipated impact conditions.
3. The fuze response is less than 25 microseconds at an impact velocity of 600 meters per second against aluminum targets.

Recommendations

The outstanding results achieved during this project warrant further development of the base fuze design. Specifically, the following tasks are recommended:

1. Integrate the design with a suitable safing and arming (S&A).
2. Prepare a design of the integrated S&A device that is compatible in size and configuration with the 30MM projectile.
3. Fabricate prototype hardware for test and evaluation.

REFERENCES

1. "Final Report on the Concept Formulation of the Avco High Performance Artillery and Mortar Point Detonating Fuze," Avco Systems Division, Contract No. DAAA-21-70-C-0040, July 1971.
2. M. Barron, HDL, private communication.
3. D. Berlincourt and H. H. A. Krueger, "Domain Processes in Lead Titanate Zirconate and Barium Titanate Ceramics," *Journal of Applied Physics*, 30, 11, 1804 (1959).
4. D. Berlincourt, H. H. A. Krueger, and B. Jaffe, "Stability of Phases in Modified Lead Zirconate with Variation in Pressure, Electric Field, Temperature and Composition," *Phys. Chem. Solids*, 25, 659 (1964).
5. D. Berlincourt, H. Jaffe, H. H. A. Krueger, and B. Jaffe, "Release of Electric Energy in $\text{PbNb}(\text{Zr}, \text{Ti}, \text{Sn})\text{O}_3$ by Temperature and by Pressure-Enforced Phase Transitions," *Applied Physics Letters*, 3, 5, 90 (1963).
6. J. Harvel, Eagle Picher Industries, Inc., private communication.
7. W. J. Halpin, "Current from a Shock-Loaded Short-Circuited Ferroelectric Ceramic Disk," *Journal of Applied Physics*, 37, 1, 153 (1966).
8. R. K. Linde, "Depolarization of Ferroelectrics at High Strain Rates," *Journal of Applied Physics*, 38, 12, 4839 (1967).
9. P. C. Lysne, "Dielectric Breakdown of Shock-Loaded PZT 65/35," *Journal of Applied Physics*, 44, 2, 577 (1973).
10. "Proceedings of Piezo²electric and Pyroelectric Symposium-Workshop," coordinated by M. F. Broadhurst, National Bureau of Standards, Report No. NBSIR75-760, September 1975.
11. P. E. Bloomfield, "Piezoelectric Polymer Films for Fuze Applications," National Bureau of Standards, Report No. NBSIR 75-724(R), August 1975.

12. N. Murayama, K. Nakamura, H. Obara, and M. Segawa, "The Strong Piezoelectricity in Polyvinylidene Fluoride," *Ultrasonics*, 14, 1, 15 (1976).
13. L. N. Bui, J. H. Shaw, and L. T. Zitelli, "Study of Acoustic Wave Resonance in Piezoelectric PVF₂ Film," *IEEE Transactions on Sonics and Ultrasonics*, SU-24, 5, 331 (1977).
14. K. Nakamura and Y. Wada, "Piezoelectricity, Pyroelectricity, and the Electrostriction Constant of Poly (vinylidene Fluoride)," *Journal of Polymer Science: Part A-2*, 9, 161 (1971).
15. M. Tamura, K. Ogasawara, N. Ono, and S. Hagiwara, "Piezoelectricity in Uniaxially Stretched Poly (vinylidene Fluoride)," *Journal of Applied Physics*, 45, 9, 3768 (1974).
16. J. Cohen and S. Edelman, "Direct Piezoelectric Effect in Polyvinylchloride Films," *Journal of Applied Physics*, 42, 2, 893 (1971).
17. S. Edelman, L. R. Grisham, S. C. Roth, and J. Cohen, "Improved Piezoelectric Effect in Polymers," *The Journal of the Acoustical Society of America*, 48, 5 (Part 1), 1040 (1970).
18. H. Ohigashi, "Electromechanical Properties of Polarized Polyvinylidene Fluoride Films as Studied by the Piezoelectric Resonance Method," *Journal of Applied Physics*, 47, 3, 949 (1976).
19. G. Pfister, M. Abkowitz, and R. G. Crystal, "Pyroelectricity in Polyvinylidene Fluoride," *Journal of Applied Physics*, 44, 5, 2064 (1973).
20. E. L. Church, H. A. Jenkinson, and R. J. Esposito, "Plastic Piezoids for Fuze Applications," *Ballistics*, 1, 183 (1977).

DISTRIBUTION LIST

Commander	
US Army Armament Research and Development Command	
ATTN: DRDAR-SC /Mr. W. Warren	3
DRDAR-TSS	5
DRDAR-QAA-R	1
Dover, NJ 07801	
Defense Documentation Center	12
Cameron Station	
Alexandria, VA 22314	